Dear Editor,

Please find attached a revised version of the typeset LaTex file of our manuscript published in BGD: *The relative importance of phytoplankton aggregates and zooplankton fecal pellets to carbon export: insights from free-drifting sediment trap deployments in naturally iron-fertilised waters near the Kerguelen plateau*.

We thank the anonymous reviewers for their valuable comments which have helped improve the manuscript. We modified the text, tables and figures according to the referee comments, optimised figure clarity and updated the references (e.g. from the discussion papers in BGD to the final papers in Biogeosciences).

All changes are detailed in our responses to the anonymous referees (attached to this document and submitted online to the interactive discussion on the 13th of December 2014). In addition, a *latexdiff* output file showing the alterations made to the manuscript is attached. Changes made to the tables do not appear in this document because of their complexity (errors generated during the typeset operation of the *latexdiff* output file). Please refer to the revised *.pdf* file for details on these modifications.

With our best regards, we thank you for your time and consideration,

E. C. Laurenceau-Cornec.

Dear editor,

We thank the anonymous referees for their thorough comments, which helped improve our manuscript. Please find below our responses carefully addressed to each comment and following the sequence: (i) comment from the referee (in italic), (ii) authors response, (iii) modification made to the manuscript.

Responses to anonymous referee #1

Comment received and published: 2 October 2014

General comments

Comment #1:

(i) *A short comment on your study design: You deployed PPS3/3 sediment traps first to determine the POC flux and then compare the POC flux directly with the POC flux estimated from the particle composition of the gel traps (deployed after recovery of the PPS3/3 traps). I am very well aware of the logistical challenges when deploying free- drifting sediment traps, but my own experience from the Barents Sea however indicates a high patchiness in phytoplankton and zooplankton distribution and a frequently higher POC flux in free-drifting sediment traps (KC Denmark) deployed for 4-5 h compared to subsequently deployed traps for 24 h (data from the Barents Sea – Wiedmann et al. 2014, JGR: Oceans, In Press – and a fjord at the Western Coast of Svalbard, unpublished data). Similar challenges may exist in your data set (13638, section 3.3, line 12-13; 13639, section 4.1, line 7-9)? For further studies, you may therefore consider to deploy gel traps and sediment traps together (if technically possible) to be really able to compare the two different ways to estimate the POC flux.*

(ii) We agree with this comment. We are aware of the potential biases that a high patchiness in phytoplankton and zooplankton distributions can cause to the evaluation of particle fluxes collected in gel and standard free-drifting sediment traps. At each station, our decision to combine or not the deployment of gel and PPS3/3 traps was first constrained by the logistic (as noted by the referee#1), but also by the required different durations of deployment for each kind of trap. The PPS3/3 traps, were deployed over an average of 3.5 days to provide sufficient material for the bulk chemical analyses, while the gel traps were deployed over an average of 1.2 days to avoid an overloading of the gels (p 13631, lines 5-6), which would have complicated considerably the image analysis and decrease its accuracy. As a consequence, at a same station, most of our separate deployments of gel and PPS3/3 traps were of different duration but were overlapping in time and space to collect the same particle fields. Our only gel and PPS3/3 trap combined deployment presented the same differences in POC flux estimations from the two collection methods suggesting that another factor might play as we discussed in section 4.1 (p 13639, lines 9-14).

(iii) We added a sentence p. 13631 line 9 to explain our deployment strategies: "Due to different required deployment duration (shorter for gel traps to avoid overloading, see above), each category of trap was deployed on separate arrays, except at A3-2 (combined deployment; Table 1). All separated deployments of gel and PPS3/3 traps overlapped in time and location (except at station E-3 where they were successive), to maximize the collection of similar particle fields. The arrays had broadly..."

Comment #2:

(i) *In your analysis, you exclude large, rare particles due to statistical reasons. I understand absolutely your decision, but you may also take into account that these large, rare particles may stand for a substantial carbon transport. We just conducted a similar study in the Barents Sea (Wiedmann et al., 2014, JGR: Oceans, In press) and including the rare, large particles improved our results substantially (POC: volume ratio of the sinking material under different physical and biological situations then met the literature values of fecal pellets or diatom aggregates). Large, rare particles may be worth considering.*

(ii) We did not exclude the large rare particles from our POC flux estimations. The large rare particles have been excluded only from our spectrum analyses which required a binning of the particles. As noted in page 13634, lines 25-28, the bins containing 5 or fewer particles were not included in the analysis for statistical reasons. All POC flux estimations, however, included all the particles except the very small unidentifiable particles potentially deriving from small gel imperfections (p 13633, lines 21-23). We apologise for this confusion due to a probably too unclear description of our image analysis method. We agree that not including these rare large particles could have led to a significant misestimation of the carbon flux.

(iii) Page 13634, line 26: we changed "... fewer particles were not included in the analysis, ..." to "... fewer particles were not included in the flux spectrum analyses, ...".

Comment #3 (part1):

(i) *I would appreciate, if the authors describe more clearly, at which stage of the spring bloom they expected to meet at the different sampling station of KEOPS II. Section 2.2 gives a coarse characterization of the different stations (may be it would be more natural to place it in the results section?), but for me, not knowing the study area, it is however very difficult to decide the bloom stage based on the presented details.*

(ii) Bloom stages encountered at the different stations during the sampling is a central question of the KEOPS2 project and presents a very high interest for the whole community. A phytoplankton community sampled at one station can possibly be an early stage of a local bloom or a later stage of a distant bloom initiated at another location and then advected. As a consequence, address this question needs to consider several complex parameters: the age of the water masses since iron-fertilisation at a sampling time and location and thus implies an accurate knowledge of the water mass circulations (d'Ovidio et al., 2014; Zhou et al., 2014), iron supply modes (Sanial et al., 2014), and sources (van der Merwe et al., 2014; Quéroué et al., 2014; Bowie et al., 2014), potentially responsible for the various phytoplankton assemblages encountered at each stations (M. Lasbleiz, personal communication; Armand et al., unpublished data). Moreover, deriving bloom stages from these parameters is still insufficient due to observed contrasted plankton community responses to natural iron fertilization (Trull et al., 2014; Sackett et al., 2014; Closset et al., 2014).

Unfortunately, it was far beyond the scope of this study to build this overview of the extremely complex spatio-temporal dynamic of the KEOPS2 blooms, requiring a thorough synthesis of the KEOPS2 dataset.

(iii) p. 13629, line 11, we added: "For more information on the complex spatio-temporal evolution of the phytoplankton bloom over the full 2011-2012 annual cycle, we refer the reader to an animation of NASA MODIS Aqua chlorophyll images that can be found as a supplementary material in (Trull et al., 2014)."

Comment #3 (part2):

(i) *Providing numbers instead of only a list of dominant species (Table 6) may here also help, as well as including Ez 1%. In addition, sampling at station E-1 to E-5 took place during a period of three weeks and I wonder if you observed any succession during this time? I assume so (13636, line 3-4, 13643, line 1-3: "temporal evolution of the flux between E-1, E-*

3, E-5."), but clarification would make it easier to follow and help to explain your data (the shift from a high to a low e-ratio at these stations). It would also be very interesting to include these stations in the discussion, instead of only focusing on R-2 and A3-2.

(ii) The 1% PAR Ez is presented on Figure 2, with other water column properties. Indeed, we observed changes in phytoplankton community at E-stations. They are attested by the increase at E-5 of the biomass of the small *Chaetoceros* subgenus *Hyalochaete* (22.5% of the diatom community) which was less represented at E-1 (10%) and E-3 (2.3%).

(iii)

- In Table 6, we added the fraction (%) represented by the dominant diatom species at each station (column "Diatom community").
- p. 13645, line 25, we added "... will be discussed in detail here..."
- p. 13646, line 11, we added: "At E-stations, used as a time series, the net primary productivity was moderate (Cavagna et al., 2014), and a shift from a high e-ratio at E-1 to a low e-ratio at E-5 was associated with plankton community shifts (e.g. increase of *Chaetoceros* subgenus *Hyalochaete* biomass at E-5; Table 6).
- p. 13646, line 12, we rephrased the sentence to: "At stations R-2 and A3-2, although presenting..."

Detailed comments

Introduction

Comment #1:

(i) *A definition of "fecal aggregates" the first time you mention it would help your reader to understand what you are talking about.*

(ii) - (iii) Thank you for drawing our attention on this omission. We added a short definition of "fecal aggregates" on page 13627 line 18: "... copepod fecal detritus (intact or degrading pellets and fecal material re-agglomerated with phytodetritus, called hereafter "fecal aggregates")

Material and methods

Comment #1:

(i) *13629, line 11: "...varying biomass levels..." Do you think here about "Chl a surface levels" or about biomass in general?*

(ii) Every use of the word "biomass", without any precision refers to the general biomass (i.e. including phytoplankton, zooplankton, etc.) and is described by POC concentrations (fig. 2).

(iii) p. 13629, line 11, we replaced "...varying biomass levels (Fig. 1)" by "...varying biomass and surface Chl. *a* levels (Fig. 1 and 2)".

Comment #2:

(i) *13630: How did you define the mixed layer? As the temperature curve in Fig. 1 is not further discussed in the paper, you may present a density curve here instead and document the mixed layer depth in this way in a more detailed way*

(ii) The mixed layer was defined by Y. Park et al. using the density difference criterion of 0.02 σ_θ (Park et al., 1998):
MLD is the depth where the potential density = potential density at 10m + 0.02 Kg m^{-3}. The value presented here at each station are averages of all CTD casts at this station. We agree that a density curve is more suited here to illustrate the water column structure.

(iii) Fig. 2, we replaced the temperature curve by a potential density curve.

Comment #3:

(i) *13632, line 19: "10 per gel" instead of "10 by gel"?*

(ii) - (iii) Certainly, thanks. We changed "10 by gel" to "10 per gel".

Comment #4:

(i) *13632, line 26: Can you describe a bit more in detail how you conducted this preliminary image analysis?*

(ii) The preliminary image analysis consisted in a binary conversion of the images and a determination of the morphological characteristics of the most represented categories of particles collected in all gels. The tests on particle area alteration from threshold and correct identification from a set of shape descriptors were also part of this phase of our work.

(iii) To improve the clarity of this paragraph, the following changes have been made:

- p. 13632, lines 26-27 was changed to "A preliminary image analysis was conducted to select the best analysis method in term of particle identification. The particles were classified into three main categories based on...".
- p. 13633, lines 4-5: "Particle characteristics were then determined by conversion to" was replaced by "Pictures were converted to".
- p. 13634 lines 27-28: "All particle characteristics investigated in this study and their units are reported in Table 2." was moved to p. 13633 line 20, to mark the begining of the actual image analysis presented here.

Comment #5:

(i) *13633, line 26: I am a bit unsure if I understand this sentence right: You assumed a) a spherical shape for the aggregates and computed the volume from the ESD, (does this mean V= 4/3 * (ESD/2)^3 * pi?) b) and a cylindrical shape for the cylindrical fecal pellets (Why did you calculate the cylinder section in exactly this way?) Did you also use an ellipsoidal volume calculation? (It is included in Table 2)*

(ii) a) yes, we used the formula *V= 4/3 * (ESD/2)^3 * pi*, to calculate our aggregate volumes assuming spherical shapes; b) yes, we assumed a cylindrical shape for the cylindrical fecal pellets.
The best fitted ellipse determined by Image J, was used to access to particle lengths and calculate the ESD. Because of their frequent "V" shape (not straight), this method could not be used to accurately measure cylindrical fecal pellet volumes. We used the fecal pellet area and perimeter (independant from the "V" or straight shape of the pellets), and calculated the radius using the formula (1) p. 13634, and the length using the formula (2) p. 13634.

(iii) p. 13633, line 28: we added "...not always straight, their volume could not be accurately measured directly from their length, and was calculated...".

Comment #6:

(i) *13634, line 12: Writing "Figure 4, Line 2" also would make it easier to understand for the reader, where to look for line 2.*

(ii)-(iii) Certainly. We added "Fig. 4" to each reference to the lines displayed on this graph.

Results

Comment #1:

(i) *13636, line 16-19: "At all sites, most of the volume flux of phytodetrital material was carried by middle sized particles". I was just curious on which data you base this sentence – I assume you use the maxima in Figure 7? According to Jackson (Deep-Sea Research I (1997) Vol 44, No 11, pp. 1739-1767, Figure 13), I think that you would have to divide the volume flux by the image diameter to make the area under the curve proportional to the volume flux. I suggest having a look at that, as it might change your results.*

(ii) - (iii) We think that a mistake was made here. We already divided our volume flux by the image diameter, (the difference between the upper and lower diameter defining the bin width), as done previously in similar studies of the volume flux spectra or volume spectra (Jackson et al., 1995; Iversen et al., 2010; Ebersbach et al., 2011). In our figure 7 we divided the volume flux spectra (expressed in $cm^3\ m^{-2}\ d^{-1}$) by the bin width (cm) to obtain units in $cm^{-3}\ m^{-2}\ d^{-1}\ cm^{-1}$. This normalisation is needed to remove the effect of bin width variations accross the whole size range; the bin are logarithmically spaced to account for the decrease of the number of particles collected when size increases (McDonnell and Buesseler, 2010).

Discussion

Comment #1:

(i) *13643, line 15: A "." is lacking after the bracket*
(ii) - (iii) We added the missing full stop.

Comment #2:

(i) *13643, line 25-29: Are these statements deduced from the results of the present work or they general statements? Please give some references*
(ii) - (iii) This statement refers to the fact that the ^{234}Th method averaged the carbon flux over a longer time period than the trap deployments. All these time averages and their citations are already indicated on p. 13643 lines 15-24.

Comment #3:

(i) *13644, line 5: Please state what Ez stands for.*
(ii) - (iii) We added "Euphotic zone" inside the brackets.

Comment #4:

(i) *13644, line 13-15: "carbon export efficiencies up to 10 fold lower during the early (spring) than late bloom stage (summer)": I have difficulties to reconstruct on which data you base this argument on. Could you please clarify it?*
(ii) - (iii) It is a comparison between the KEOPS1 and 2 data of the carbon export efficiency. The data and their references are indicated on the previous sentence (p. 13644 lines 6-11).

Comment #5:

(i) *13646, line 12 and following: You state that physical aggregation seemed to dominate over the biological aggregation, due to the rarity of fecal pellets. This appears a*

very general statement to me. Please include more details, which kind of physical processes you would suggest to dominate in aggregate formation and why? In the following you start a paragraph on the inverse relationship between net primary productivity and export efficiency, which is in my opinion a very interesting topic. However, your discussion of this observation is rather difficult to read (long sentences) and ends unfortunately a bit pointless. I would suggest rewriting this paragraph, and possibly including ballasting effects/ different abilities of the microalgae to produce EPS as "natural glue" for the aggregates/...?

(ii) p. 13646, line 12: This sentence is a transition between the previous paragraph and the next. The statement of the dominance of physical aggregation (i.e. forming phytodetrital aggregates and fecal aggregates) over biological aggregation (i.e. forming fecal pellets) at stations R-2 and A3-2 is inferred from p. 13645, line 27 to p. 13646, line 11.

The next paragraph (p. 13646, lines 17-21), cites aggregation experiments conducted at six stations over and downstream the Kerguelen plateau (Laurenceau-Cornec et al., In press, 2014). This study focused on the influence of contrasted phytoplankton morphologies accross species variations on physical aggregation processes, resulting phytodetrital aggregate structures and sinking velocities. This article includes the investigations on potential ballast effect and TEP importance in aggregation processes suggested by reviewer#1.

We did not address these perspectives here since they are largely developed in Laurenceau-Cornec et al. (in press, 2014). We agree that reference to this work should occur earlier in this paragraph and more clearly.

We acknowledge that the discussion on the relationship between phytoplankton aggregate sinking velocities and carbon export efficiencies (p. 13646 lines 17-29), lacks of evidence at this stage. The evocation of the work from Laurenceau-Cornec et al. is however essential to discuss the potential role of the physical aggregation on contrasted export efficiencies. We understand that concluding that these experiments, unfortunately cannot be used here to explore this aspect any further is disappointing.

However, our discussion on the inverse relationship between primary production and carbon export does not end on p. 13646 line 29, but on p. 13648 line 4, providing the reader with other hypotheses.

(iii) p. 13646, line 17-21: we changed this sentence to: "In parallel of this study, roller tank experiments have been conducted to explore the influence of different phytoplankton communities on physical aggregation forming the phytodetrital aggregates and on their sinking velocities (Laurenceau-Cornec et al., 2014). These experiments consisted in the physical aggregation of natural assemblages sampled with Niskin bottles at high and low biomass sites during KEOPS2. The results suggest that the proportions of different phytoplankton types forming the phytodetrital aggregates could influence their sinking velocity (and potentially their efficiency at exporting carbon), via a control on their structure and excess density. However, ..."

Comment #6:

(i) *13647, line 1-9: "...unexpected high export efficiency considering its high zooplankton biomass". Zooplankton is doubtless an important factor in carbon attenuation, but they also can produce fast-sinking pellets, and contribute to an enhanced POC flux. You might include this.*

(ii) p. 13647, lines 6-9: we wrote "In this perspective, however, E-3 presented ...". We do agree that the usual view is that zooplankton, via fast-sinking pellets is an important contributor to the carbon flux. Here, we explore the possibility that this mechanism does not always prevail and that zooplankton grazing associated with a degradation of fecal pellets at depth could make zooplankton grazing as a factor potentially reducing the carbon export and possibly explaining the inverse relationship between primary production and carbon export.

(iii) We moved our hypothesis of a zooplankton grazing reducing the carbon export p. 13647 lines 10-13 "In the case ... Iversen and Poulsen, 2007)" to p. 13647 line 2.

Conclusion

Comment #1:

(i) *Conclusion 1 is absolutely right, however I think it is important to also point out that the conversion to carbon makes fecal pellets to an important carbon flux vehicle (as named in the abstract).*

(ii) - (iii) We added p. 13648, line 11: "However, when converted to carbon content, and where their degradation was limited, cylindrical fecal pellets still represented the dominant fraction of the flux."

Comment #2:

(i) *Conclusion 2: "The decrease of productivity..." You may add "from KEOPS 1 and the present study" to clarify that these are your results and not a general statement ..."shift from autotroph to heterotroph-dominated regimes": Is this shown in your study, a KEOPS 1 vs. KEOPS 2 result or a general statement? Please state it more clearly.*

(ii) The "shift from autotroph to heterotroph-dominated regimes" refers to the modes of carbon export either via phytodetrital aggregates (autotroph-dominated regime observed during KEOPS2) or fecal material (heterotroph-dominated regime observed during KEOPS1).

(iii) p. 13648, line 15: We added: "The decrease of productivity from bloom initiation (KEOPS2) to its decline (KEOPS1), related to a shift from autotroph- to heterotroph-dominated regimes (i.e. production exported via phytodetrital vs fecal material), could explain..."

Comment #3:

(i) *Conclusion 3: You may use "appear to" instead of "could"? Conclusion 3 is very general, and I miss a bit the relation to you study. May be you would like to change it to something that is more specific for your study – perhaps that you observed more phytoplankton aggregates and fecal aggregates at depth?*

(ii) This last conclusion is intentionally very general. It refers to the discussion relating plankton (phyto- and zoo-) communities to the productivity regimes observed at different stations (high vs low) and contrasted carbon export efficiency. This discussion is detailed from p. 13645 line 19 to p. 13647 line 20 and uses Table 6 as main support.

(iii) p. 13648 line 19, we added: "... and zooplankton grazing pressure (Table 6)".

Comments on Tables

Table 2:

(i) *Was your 10th bin actually including all larger particles since it has no upper limit?*

(ii) - (iii) Yes, this bin has no upper limit and included all particles with an esd bigger than 0.1752. As detailed on general comments (comment #2), our study excluded particles from the spectrum analyses only if 5 or fewer particles were included in a bin.

Table 5 - comment 1:

(i) *Minimum export efficiencies in italic are rather difficult to find. May be underlined numbers would be better?*

(ii) - (iii) Maximum and minimum export efficiencies are now both indicated in bold.

Table 5 - comment 2:

(i) *The maximum e-ratio of 0.32 is in bold, but not the e-ratio of 0.34. Was this on purpose?*

(ii) - (iii) We fixed this error. The highest e-ratio at E-1, 200m, is now in bold.

Table 5 - comment 3:

(i) *Footnotes: Some of the abbreviations presented here are not used in the table*

(ii) - (iii) These are notations from a previous version of this table. Thank you for signaling this mistake. We removed "PA, CFP, FA, O and Ez".

Table 6 - comment 1:

(i) *Include full name of T. nitzschoides once.*

(ii) - (iii) We added the full name at its first reference in the Table (site R-2, column "Diatom community").

Table 6 - comment 2:

(i) *Would be very interesting to include the depth of the euphotic zone here as well as numbers of phytoplankton and zooplankton.*

(ii) - (iii) We made the following changes to Table 6:

- we added a column for the mixed layer and euphotic zone depths.
- we added the relative fractions of the total diatom community represented by each diatom genera or species displayed in Table 6, column "Diatom community"
- we added the relative fractions of the total biomass represented by the mesozooplankton groups, genera or species displayed in the column "Mesozooplankton community"

Table 6 - comment 3:

(i) *A3-2: "Appendicularians" should be in one line.*

(ii) - (iii) Thank you for signaling this error introduced during the production process. The word "Appendicularians" now appears on the next line after "*Paraeuchaeta* sp. C1-C3".

Table 6 - comment 4:

(i) *"sp." not in italics.*

(ii) - (iii) All "*sp.*" have been put in regular style.

Comments on Figures

Figure 2:

(i) *Unsure about the unit "µm L^-1" for fluorescence. Perhaps you should use "Chl a" instead?*

(ii) - (iii) The parameter displayed here is the fluorescence converted to Chl. *a* values using a calibration with CTD Niskin bottle data. The new fig. 2 (modified according to general comment #2), displays now "Chl. *a*" instead of fluorescence.

REFERENCES

Bowie, A. R., van der Merwe, P., Trull, T. W., Quéroué, F., Fourquez, M., Planchon, F., Sarthou, G., and Blain, S.: Iron budgets for three distinct biogeochemical sites around the Kerguelen archipelago (Southern Ocean) during the natural fertilisation experiment KEOPS-2 Biogeosciences Discuss., 2014.

Closset, I., Lasbleiz, M., Leblanc, K., Quéguiner, B., Cavagna, A.-J., Elskens, M., Navez, J., and Cardinal, D.: Seasonal evolution of net and regenerated silica production around a natural Fe-fertilized area in the Southern Ocean estimated with Si isotopic approaches, Biogeosciences, 11, 5827--5846, 10.5194/bg-11-5827-2014, 2014.

d'Ovidio, F., Della Penna, A., Trull, T. W., Nencioli, F., Pujol, I., Rio, M. H., Cotté, C., Zhou, M., and Blain, S.: The biogeochemical structuring role of horizontal stirring: Lagrangian perspectives on iron delivery downstream of the Kergulen plateau, Biogeosciences Discuss., 2014.

Ebersbach, F., Trull, T. W., Davies, D. M., and Bray, S. G.: Controls on mesopelagic particle fluxes in the Sub-Antarctic and Polar Frontal Zones in the Southern Ocean south of Australia in summer---Perspectives from free-drifting sediment traps, Deep Sea Research Part II: Topical Studies in Oceanography, 58, 2260--2276, doi: 10.1016/j.dsr2.2011.05.025, 2011.

Iversen, M. H., Nowald, N., Ploug, H., Jackson, G. A., and Fischer, G.: High resolution profiles of vertical particulate organic matter export off Cape Blanc, Mauritania: Degradation processes and ballasting effects, Deep Sea Research Part I: Oceanographic Research Papers, 57, 771--784, 10.1016/j.dsr.2010.03.007, 2010.

Jackson, G. A., Logan, B. E., Alldredge, A. L., and Dam, H. G.: Combining particle size spectra from a mesocosm experiment measured using photographic and aperture impedance (Coulter and Elzone) techniques, Deep Sea Research Part II: Topical Studies in Oceanography, 42, 139--157, 10.1016/0967-0645(95)00009-f, 1995.

Laurenceau-Cornec, E. C., Trull, T. W., Davies, D., De La Rocha, C. L., and Blain, S.: Phytoplankton morphology controls on marine snow sinking velocity, Marine Ecology Progress Series, In press, 2014.

McDonnell, A. M. P., and Buesseler, K. O.: Variability in the average sinking velocity of marine particles, Limnology and Oceanography, 55, 2085--2096, 10.4319/lo.2010.55.5.2085, 2010.

Park, Y.-H., Charriaud, E., Pino, D. R., and Jeandel, C.: Seasonal and interannual variability of the mixed layer properties and steric height at station KERFIX, southwest of Kerguelen, Journal of Marine Systems, 17, 571--586, 10.1016/S0924-7963(98)00065-7, 1998.

Quéroué, F., Sarthou, G., Planquette, H., Bucciarelli, E., Chever, F., van der Merwe, P., Lannuzel, D., Townsend, A. T., Cheize, M., Blain, S., d'Ovidio, F., and Bowie, A. R.: High variability of dissolved iron concentrations in the vicinity of Kerguelen Island (Southern Ocean), Biogeosciences Discuss., 2014.

Sackett, O., Armand, L., Beardall, J., Hill, R., Doblin, M., Connelly, C., Howes, J., Stuart, B., Ralph, P., and Heraud, P.: Taxon-specific responses of Southern Ocean diatoms to Fe enrichment revealed by synchrotron radiation FTIR microspectroscopy, Biogeosciences Discuss., 11, 7327--7357, 10.5194/bgd-11-7327-2014, 2014.

Sanial, V., van Beek, P., Lansard, B., Souhaut, M., Kestenare, E., d'Ovidio, F., Zhou, M., and Blain, S.: Use of Ra isotopes to deduce rapid transfer of sediment-derived inputs off Kerguelen, Biogeosciences Discussions, 11, 14023--14061, 10.5194/bgd-11-14023-2014, 2014.

Trull, T. W., Davies, D. M., Dehairs, F., Cavagna, A.-J., Lasbleiz, M., Laurenceau-Cornec, E. C., d'Ovidio, F., Planchon, F., Leblanc, K., Quéguiner, B., and Blain, S.: Chemometric perspectives on plankton community responses to natural iron fertilization over and downstream of the Kerguelen Plateau in the Southern Ocean, Biogeosciences Discussions, 11, 13841--13903, 10.5194/bgd-11-13841-2014, 2014.

van der Merwe, P., Bowie, A. R., Quéroué, F., Armand, L., Blain, S., Chever, F., Davies, D., Dehairs, F., Planchon, F., Sarthou, G., Townsend, A. T., and Trull, T.: Sourcing the iron in the naturally-fertilised bloom around the Kerguelen Plateau: particulate trace metal dynamics, Biogeosciences Discussions, 11, 13389--13432, 10.5194/bgd-11-13389-2014, 2014.

Zhou, M., Zhu, Y., d'Ovidio, F., Park, Y.-H., Durand, I., Kestenare, E., Sanial, V., Van-Beek, P., Queguiner, B., Carlotti, F., and Blain, S.: Surface currents and upwelling in Kerguelen Plateau regions, Biogeosciences Discuss., 11, 6845--6876, doi: 10.5194/bgd-11-6845-2014, 2014.

Dear editor,

We thank the anonymous referees for their thorough comments, which helped improve our manuscript. Please find below our responses carefully addressed to each comment and following the sequence: (i) comment from the referee (in italic), (ii) authors response, (iii) modification made to the manuscript.

Responses to anonymous referee #2

Comment received and published: 23 October 2014

General comments

Comment #1:

(i) *PPS3/3 and gel-cups were not simultaneously deployed. This situation might be a problem because the authors made comparisons based on similar nutrient and plankton scenarios, which is not necessarily true.*

(ii) We are aware of the potential biases that a high patchiness in phytoplankton and zooplankton distributions can cause to the evaluation of particle fluxes collected in gel and standard free-drifting sediment traps. Our Table 1 shows that only one station (E-3), was sampled by a non-synchronised trap deployment. At all other stations, the deployments were either single deployments of gel or PPS3/3 traps (R-2 and F-L), deployments overlapping in time and space (E-1 and E-5) or combined deployments of gel and PPS3/3 traps (A3-2).

At each station, our decision to combine or not the deployments was first constrained by the logistic, but also by the required different durations of deployment for each kind of trap. The PPS3/3 traps, were deployed over an average of 3.5 days to provide sufficient material for the bulk chemical analyses, while the gel traps were deployed over an average of 1.2 days to avoid an overloading of the gels (p 13631, line 6), which would have complicated considerably the image analysis and decrease its accuracy. Most of our separate gel and PPS3/3 trap deployments were in the same temporal and spatial field and likely collected particle fields originating from similar nutrient and plankton ecosystem structures.

Moreover, the core of the informations extracted from the gel or the PPS3/3 were of different nature: qualitative in the case of the gel collection and quantitative in the case of PPS3/3 traps as noted p. 13628 line 20 to p. 13629 line 3. We compared POC fluxes from gel and PPS3/3 traps in the perspective of a method comparison rather than to infer our main conclusions in term of relative importance of the different category of particles in carbon export flux.

Actually, the fluxes collected by the gel and PPS3/3 at every station compared relatively well, considering how far these methods are. This good match tends to suggest that our gel and PPS3/3 traps effectively collected similar flux episodes.

(iii) As also requested by referee#1, we added a sentence p. 13631 line 9 to explain our deployment strategies: "Due to different required deployment duration (shorter for gel traps to avoid overloading, see above), each category of trap was deployed on separate arrays, except at A3-2 (combined deployment; Table 1). All separated deployments of gel and PPS3/3 traps overlapped in time and location (except at station E-3 where they were successive), to maximize the collection of similar particle fields. The arrays had broadly..."

Comment #2:

(i) *The authors mention that the average trap drift speed was 8.5 cm s^{-1} and I wonder whether the authors can provide with consistent evidence and information that this situation did not affect significantly the trap collection efficiency. In the study area the current speed along the slope and shelf break can be significantly higher.*

(ii) - (iii) In p. 13631 lines 16-18, we wrote: "The average trap drift speed of 8.5 ± 5 cm s^{-1} was in the range of horizontal velocities determined by drogued drifter trajectories (Zhou et al., 2014). This is a strong evidence of a limited perturbation due to currents.
Moreover, the limited tilts recorded by the inclinometer (p. 13631 lines 18-20), attest that particle collection efficiency was not reduced by the current speed. This information tends to demonstrate that even in higher current areas that the traps could have potentially met, they always kept a satisfying semi-vertical position ensuring an efficient collection of the sinking flux at a given location and time.
An additionnal indication is given by the aspect and repartition of the particles embedded in the polycacrylamide gels (fig. 3 and 5): no evidence was found of major particle deformation, heterogeneous collection or gel flow which would have testify of perturbation due to hydrodynamic conditions.

Comment #3:

(i) *Fecal and phytodetrital aggregates were distinguished because fecal matter was more dense and compact and phytodetritus loose and green, which seems to be a rather subjective criteria. Some observations using both light and electron microscopy probably would help to dissipate doubts?. The authors isolated fecal aggregates manually to conduct some tests, but from the text it is not clear enough which kind of test you did to be sure that fecal and phytodetritus-aggregates were correctly classed.*

(ii) Sorry for the confusion. This section needs to be rewritten more clearly to reflect accurately the different steps of our image analysis.
Polyacrylamide gels were studied exclusively using image analysis of light microscopy pictures. A method permitting electron microscopy on marine particles embedded in polyacrylamide gels is unfortunately not yet developed.
All the fecal material, including fecal aggregates and fecal pellets together (not mentioned in the MS and probably source of the confusion), has been isolated manually from the "total" images (displaying all the particles). "Manually" means that fecal particles were isolated with an Image J selection tool based on the assumption that fecal matter is brown and denser as noted p. 13633 lines 16-17 and showed on figure 3.
Two sets of images have been obtained: (1) the images containing only the fecal matter (fecal aggregates + fecal pellets), and (2), the images containing all remaining particles composed mainly of phytodetrital aggregates. Using a combination of shape parameters each category of particle wanted for the flux analysis (fecal aggregates, cylindrical fecal pellets, phytodetrital aggregates) have been selected automatically in these two sets of images through Matlab routines. The objective was to isolate manually particles impossible to separate automatically due to very similar shapes (fecal and phytodetrital aggregates) and group particles easy to separate automatically (fecal aggregates can be easily separated from fecal pellets due to their very different shapes).

(iii) p. 13633 lines 14-20, we rewrote this paragraph: "Because fecal and phytodetrital aggregates had similar complex shapes, automated routines could not separate these particles efficiently. All fecal material was thus isolated manually from all other particles based on the assumption that fecal matter is brown and denser than biologically unprocessed phytoplankton (Ebersbach et al., 2011). From the resulting set of pictures, fecal aggregates were separated easily from cylindrical fecal pellets due to their very contrasted shapes. Tests on the efficiency of our automated selection, conducted on a large sample, showed that ..."

Comment #4:

(i) *The high phytodetritus coincide with high abundance of diatoms (as indicate by the biogenic-silica concentration), but no comments on the physiological state of the diatoms we included in the text. Did you notice that diatoms or the other functional groups of the phytoplankton were in relatively bad physiological condition? It would be interesting to have some comments on this situation that have been also reported for upwelling areas (Progress in Oceanography 83: 217-227; 2009).*

(ii)

- PDMPO labelling (Shimizu et al., 2001) on diatoms has been conducted during KEOPS2 (K. Leblanc, MIO, Marseille, France). This fluorescent probe marks the silica actively deposited and thus can be used as an indicator of cell physiological state (Leblanc et al., 2005). The definitive results are not yet available but preliminary analyses show that diatoms at all sites over the Kerguelen plateau showed in general a good level of marking by the PDMPO, suggesting an active silicification during KEOPS2.

- M. Lasbleiz (personal communication, 2014) found a relatively high proportion of alive compared to empty diatom cells, even at very low PAR levels, which tends to suggest a good physiological state at this period of the season: R-2 (116 m, 0.3% PAR): 81%; E-1 (80 m, 0.3% PAR): 70%; E-3 (137 m, 0.01% PAR): 41%; E-5 (110 m, 0.01% PAR): 45%; F-L (52 m, 0.01% PAR): 92%; A3-2 (151 m, 0% PAR): 78%.

Microplankton other than diatoms showed even higher proportions of alive cells: R-2 (116 m, 0.3% PAR): 90%; E-1 (80 m, 0.3% PAR): 85%; E-3 (137 m, 0.01% PAR): 85%; E-5 (110 m, 0.01% PAR): 94%; F-L (52 m, 0.01% PAR): 87%; A3-2 (151 m, 0% PAR): 96%.

These data are preliminary results and cannot be published here.

- Moreover, the generally good physiological state of phytoplankton observed during the early bloom conditions of KEOPS2 as suggested by these results is consistant with the observed limited depletion of nitrates (Dehairs et al., 2014), and silicic acid (Closset et al., 2014).

The present study can be compared with the situation observed by (González et al., 2009), in the Humboldt Current System off Chile. González et al. (2009), suggested that the proportion of carbon exported through euphausiids fecal pellets vs diatoms depends upon the physiological state of phytoplankton. They also suggested that the carbon export mode (i.e. fecal pellets vs. phytoplankton detritus) is related to "the proportion of carbon that effectively sinks (...) compared to the carbon being fixed through GPP" (i.e. carbon export efficiency). A low export efficiency being associated with a diatom-controlled export mode (e.g. average of 32% of sinking organic matter composed of diatoms).

This relationship between the physiological state of phytoplankton and carbon export mode cannot be verififed here since, as noted above, most of the phytoplankton presented good physiological states associated to the early-stage of the bloom (limited nutrient exhaustion). Rather, we explain the variations in carbon export modes by a spatio-temporal structuration of plankton communities controlling species-dominance status and trophic interactions.

(iii) We added the following sentences to refer to the work from González et al. (2009):

- p. 13645, lines 3-5: "While this negative relationship has been observed now in several field studies in the Southern Ocean (Savoye et al., 2008; Morris et al., 2007; Jacquet et al., 2011), and elsewhere (e.g. González et al., 2009), the reasons for its existence remain unclear."
- p. 13645, line 8: "..., or increase in DOC export. Phytoplankton physiological state has also been suggested as a possible control of carbon export mode and efficiency (González et al., 2009), although this could not be verified here due to a general good phytoplankton physiological state observed via microscopy over the course of the KEOPS2 study (M. Lasbleiz and K. Leblanc, personal communication, 2014)."

Comment #4 (suite):

(i) *Laurenceau et al. suggest that high export efficiency could be mediated by fast-sinking aggregates of heavy silicified, grazing-resistant diatoms. It would be interesting whether the authors make some statements on the relevance of diatoms as triggers of high export efficiency. In other words the relationship between chain-forming diatoms and the efficiency of the biological pump in marine systems.*

(ii) We acknowledge the importance of diatoms in export efficiency and especially the influence of diatom morphology in carbon export efficiency. In this context, we refer to the work conducted by Laurenceau-Cornec et al. (in press, 2014) on the influence of phytoplankton morphology on the sinking velocity of marine snow formed from natural phytoplankton assemblages sampled in the KEOPS2 bloom. This study suggests that the proportion of large chain-forming diatoms without setae vs small setae-forming diatoms strongly influence marine snow structure and consequently sinking velocity and likely export efficiency.

(iii) p. 13646, line 21: we added the following sentence: "... via a control on their structure and excess density (Laurenceau-Cornec et al., in press, 2014). Laurenceau-Cornec et al. (2014) found a strong relationship (r^2 = 0.98) between the proportion of small spine-forming diatom cells included in marine snow aggregates (e.g. *Chaetoceros* subgenus *Hyalochaete*), and their sinking velocity, suggesting an important role for phytoplankton morphology on export efficiency."

Comment #5:

(i) *The authors speculate that the increase of phytodetrital and fecal aggregates observed at depth in some stations (E-3) could reflect an earlier production event. An analysis of the phytoplankton composition would give insight on this aspect. Whether the composition did not change significantly I did not see reasons to exclude E-3 from Fig. 6.*

(ii) We think a mistake was made here since we did not exclude station E-3 from figure 6. We assume that this comment refers mainly to p. 13642 lines 22-24 but some clarifications are needed. Does reviewer #2 refers to "phytoplankton composition" in term of phytodetritus chemical compounds as possible signature of organic matter degradation state (expected higher in case of an older production event), or in term of phytoplankton community as potential source tracer of the particle field collected in traps?
When writing "...*exclude E-3 from Fig. 6*" did the reviewer #2 referred actually to the Figure 9 caption (p. 13673): "E-3 was assumed an outlier and was excluded from the best fit calculation..."?
If suggesting an analysis of phytoplankton community or chemical compounds as a tracer of an earlier production event collected in the traps, our data need to be cross-checked with other KEOPS2 data. Unfortunately, PPS3/3 trap results cannot be used here since they provide a bulk chemical composition including all sinking organic and inorganic matter originating from auto- and heterotroph organisms. Similarly, particles collected in gel trap were only analysed in term of particle category statistics and morphologies. A determination of phytoplankton communities (genera and species if possible), collected in the gels, in the form of single or aggregated particles, or even their chemical analysis, are planned but these data are not yet available.
Assuming a steady state and a sinking velocity of the phytodetrital aggregates formed at E-3, of ~150 m day^{-1} (based on measurements reported by Laurenceau-Cornec et al., in presse, 2014), a particle field would need ~1.5 days to sink from 210 m (second shallowest trap) to 430 m (deepest trap), if neglecting any advection. This, combined with the short deployment time at E-3 (1.02 day), it is very unlikely that the deepest and shallowest traps recorded the similar production event.

(iii) p. 13642, line 22, we added:"... cup variations (Table 4). In addition, if assuming phytodetrital aggregates at E-3 sinking at an average velocity of 150 m day^{-1} (based on Laurenceau-Cornec et al., in press, 2014), a particle field would need approximately 1.5 day to sink from 210 m to 430 m, neglecting any advection. A non steady state assumption..."

Comment #6:

(i) *Large-size, rare fecal pellets or phyto-aggregates may have a disproportionate high impact in the results and final conclusions. For example, one large pellet could contribute with a large fraction of the total carbon exported and are sometime considered outlier and usually not included in the analysis. How was your criterion on this issue?*

(ii) (Same answer than to referee#1 - general comment#2) We did not exclude the large rare particles from our POC flux estimations. The large rare particles have been excluded only from our spectrum analyses which required a binning of the particles. As noted in page 13634, lines 25-28, the bins containing 5 or fewer particles were not included in the analysis for statistical reasons. All POC flux estimations, however, included all the particles except the very small unidentifiable particles potentially deriving from small gel imperfections (p 13633, lines 21-23). We apologise for this confusion due to a probably too unclear description of our image analysis method. We agree that not including these rare large particles could have led to a significant misestimation of the carbon flux.

(iii) Page 13634, line 26: we changed "... fewer particles were not included in the analysis, ..." to "... fewer particles were not included in the flux spectrum analyses, ...".

Comment #7:

(i) *During KEOPS2 a negative relationship between primary productivity and carbon export efficiency was found. So, where did the photosynthetically produced organic matter go in sites with high primary production?. Even though the processes that control export efficiency are beyond the scope of this contribution, this issue is highly relevant and I would ask the authors to provide more antecedents and insights on the possible effect of grazing or other biological/physical processes on the export mode and controls*

(ii) We agree that this question is extremely important. This is the reason why we allocated a large part (almost 40%) of our discussion (p. 13645 line 18 to p. 13648 line 4), to address it. However, acknowledging the high interest of this question and willing to address positively this comment, we put an additional paragraph in our discussion, to explore the possible pathways for the organic carbon produced at station A3 where a high primary productivity was associated with a low export efficiency. This paragraph is based on calculations using our results and results published by Christaki et al. (2014).

(iii) We made the following changes to this section:

- p. 13664, Table 6: the mesozooplankton biomass is now expressed in $mm^3\ m^{-3}$ to match with the unit used in Figure 9.
- p. 13646, line 8: the modification of zooplankton biomass unit from ind m^{-3} to mm^{-3} m^{-3} modified the ranking of A3-2. We change the sentence to: "The mesozooplankton biomass was high at A3-2".
- p. 13645, line 23: we removed the word "apparent".
- p. 13647 line 13, we modified this section and added a paragraph as follows:

"In the low productive systems (e.g. R-2), a direct export can be efficient if processed via fast-sinking aggregates composed of heavy silicified diatoms that are also assumed to be grazing-resistant. In contrast, in the sites of high productivity (e.g. A3-2 and F-L), the export flux can be strongly attenuated if a large fraction of the organic carbon flows toward paths promoting its retention in the surface layer (i.e. grazing, microbial remineralization and biomass accumulation). In the case of high grazing pressure, carbon export is driven mostly via fecal pellets, but these, even if sinking fast, potentially experience coprophagy or coprorhexy (Suzuki et al., 2003; Lampitt et al., 1990; Iversen and Poulsen, 2007), and disaggregation processes facilitating bacterial remineralization (Giering et al., 2014).

At A3, Christaki et al. (2014), proposed a carbon budget integrated over the mixed layer showing the carbon flows through microbial and higher trophic levels for early and late bloom stages. This budget indicates that during KEOPS2, 2400 mg C m^{-2} d^{-1} were still available for phytoplankton biomass accumulation or export, after substracting from the Gross Community Production (GCP), the different loss terms due to bacterial, other microplankton and mesozooplankton respiration and virus bacterial lysis. Using our carbon flux value at 200 m and phytodetrital aggregate contributions to this export, the relative fractions of the available

carbon actually used for biomass accumulation or export can be estimated here. The carbon flux at 200 m was 66 mg C m^{-2} d^{-1} (gel trap results), with 41 % contributed by phytodetrital aggregates (Table 3). This leads to 27 mg C m^{-2} d^{-1} exported (1.1% of the remaining available carbon) and 2373 mg C m^{-2} d^{-1} used for biomass accumulation (98.9%).
The same calculations can be made for the late-bloom situation using the values of 384 mg C m^{-2} d^{-1} for the carbon still available for biomass accumulation or export (Christaki et al., 2014), the KEOPS1 200 m POC flux at A3 (62 mg C m^{-2} d^{-1}; Ebersbach and Trull, 2008) and a 36% aggregate contribution (including both phytodetrital and mixed aggregates; Ebersbach and Trull, 2008). Results lead to 22 mg C m^{-2} d^{-1} exported (5.7%) and 362 mg C m^{-2} d^{-1} used for biomass accumulation (94.3%).
These estimations show that the fraction of the carbon available that is exported, is subjected to the largest variations during the season (increased by a factor ~5); while the fraction allocated to biomass accumulation varied comparatively much less (decreased by a factor of ~1.05). It suggests that A3 progressed over the whole season from a retention-dominated to an export-dominated food web system (Wassmann, 1998), possibly related to successions of plankton communities prone to large variations of their export ability, as suggested in this study.
This general picture can be compared ..."

Comment #7 (suite):

(i) *Could you speculate on the reasons why microzooplankton did not show high numbers in trap samples nor in the water column?*

(ii) In this article, we did not present data on microzooplankton abundance, but made the following statement p. 13632, line 19-21: "A few zooplankton specimens were collected (less than 10 per gel), and were mostly represented by copepods (adult and copepodite stages), appendicularians, foraminifera and radiolarians". We apologise for the confusion, the terms "few" and "10 per gel" concerned the mesozooplankton only. We identified some specimens occasionnally in high resolution observations conducted in parallel of our main survey. Due to their small size and generally uniform spherical shape, no automatic counting of these organisms was performed.

(iii) p. 13632, line 19-21, we changed this sentence: "A few mesozooplankton specimens were collected (less than 10 per gel), and were mostly represented by copepods (adult and copepodite stages), and appendicularians. Foraminifera and radiolarians were also occasionnally observed."

REFERENCES

Christaki, U., Lefèvre, D., Georges, C., Colombet, J., Catala, P., Courties, C., Sime-Ngando, T., Blain, S., and Obernosterer, I.: Microbial food web dynamics during spring phytoplankton blooms in the naturally iron-fertilized Kerguelen area (Southern Ocean), Biogeosciences, 11, 6739--6753, 10.5194/bg-11-6739-2014, 2014.

González, H. E., Daneri, G., Iriarte, J., Yannicelli, B., Menschel, E., Barría, C., Pantoja, S., and Lizárraga, L.: Carbon fluxes within the epipelagic zone of the Humboldt Current System off Chile: The significance of euphausiids and diatoms as key functional groups for the biological pump, Progress in Oceanography, 83, 217--227, 10.1016/j.pocean.2009.07.036, 2009.

Leblanc, K., Hutchins, D. A., and others: New applications of a biogenic silica deposition fluorophore in the study of oceanic diatoms, Limnology and Oceanography: Methods, 3, 462--476, 2005.

Shimizu, K., Del Amo, Y., Brzezinski, M. A., Stucky, G. D., and Morse, D. E.: A novel fluorescent silica tracer for biological silicification studies., Chem Biol, 8, 1051--1060, 2001.

Zhou, M., Zhu, Y., d'Ovidio, F., Park, Y.-H., Durand, I., Kestenare, E., Sanial, V., Van-Beek, P., Queguiner, B., Carlotti, F., and Blain, S.: Surface currents and upwelling in Kerguelen Plateau regions, Biogeosciences Discuss., 11, 6845--6876, doi: 10.5194/bgd-11-6845-2014, 2014.

Manuscript prepared for Biogeosciences Discuss.
with version 2014/09/16 7.15 Copernicus papers of the LaTeX class copernicus.cls.
Date: 16 December 2014

The relative importance of phytoplankton aggregates and zooplankton fecal pellets to carbon export: insights from free-drifting sediment trap deployments in naturally iron-fertilised waters near the Kerguelen plateau

E. C. Laurenceau-Cornec[1,2], T. W. Trull[2,3], D. M. Davies[2], S. G. Bray[2], J. Doran[4], F. Planchon[5], F. Carlotti[6], M.-P. Jouandet[6], A.-J. Cavagna[7], A. M. Waite[4], and S. Blain[8,9]

[1]CSIRO-UTAS Quantitative Marine Sciences PhD Program, Institute for Marine and Antarctic Studies, University of Tasmania, Private Bag 129, Hobart Tasmania Australia 7001
[2]Antarctic Climate and Ecosystems Cooperative Research Centre, University of Tasmania, Private Bag 80, Hobart Tasmania Australia 7001
[3]Commonwealth Scientific and Industrial Research Organisation, Marine and Atmospheric Research, Castray Esplanade, Hobart Tasmania Australia 7000
[4]UWA Oceans Institute, The University of Western Australia (M470), 35 Stirling Highway, Crawley Western Australia Australia 6009
[5]Laboratoire des Sciences de l'Environnement Marin (LEMAR), Université de Brest, CNRS, IRD, UMR6539, IUEM; Technopôle Brest Iroise, Place Nicolas Copernic, 29280 Plouzané, France
[6]Mediterranean Institute of Oceanography (MIO), Aix-Marseille Université, CNRS-IRD, 13288 Marseille, Cedex 09, France

[7]Vrije Universiteit Brussel, Analytical and Environmental Geochemistry dept., Brussels, Belgium
[8]CNRS, UMR7621, LOMIC, Observatoire Océanologique, 66650 Banyuls-sur-Mer, France
[9]UPMC Université Paris 06, UMR7621, LOMIC, Observatoire Océanologique, 66650 Banyuls-sur-Mer, France

Correspondence to: E. C. Laurenceau-Cornec (emmanuel.laurenceau@utas.edu.au)

Abstract

The first KErguelen Ocean and Plateau compared Study (KEOPS1), conducted in the naturally iron-fertilised Kerguelen bloom, demonstrated that fecal material was the main pathway for exporting carbon to the deep ocean during summer (January–February 2005), suggesting a limited role of direct export via phytodetrital aggregates. The KEOPS2 project re-investigated this issue during the spring bloom initiation (October–November 2011), when zooplankton communities may exert limited grazing pressure, and explored further the link between carbon flux, export efficiency and dominant sinking particles depending upon surface plankton community structure. Sinking particles were collected in polyacrylamide gel-filled and standard free-drifting sediment traps (PPS3/3), deployed at six stations between 100 and 400 m to examine flux composition, particle origin and their size distributions. Results revealed an important contribution of phytodetrital aggregates (49 ± 10 % and 45 ± 22 % of the total number and volume of particles respectively, all stations and depths averaged). This high contribution dropped when converted to carbon content (30 ± 16 % of total carbon, all stations and depths averaged), cylindrical fecal pellets representing then the dominant fraction (56 ± 19 %).

At 100 and 200 m depth, iron and biomass enriched sites exhibited the highest carbon fluxes (maxima of 180 and 84 ± 27 mg C m^{-2} d^{-1}; based on gel and PPS3/3 trap collection respectively), especially where large fecal pellets dominated over phytodetrital aggregates. Below these depths, carbon fluxes decreased (48 ± 21 % decrease in average between 200 and 400 m), and mixed aggregates composed of phytodetritus and fecal matter dominated, suggesting an important role played by physical aggregation in deep carbon export.

Export efficiencies determined from gels, PPS3/3 traps and ^{234}Th disequilibria (200 m carbon flux/net primary productivity), were negatively correlated to net primary productivity with observed decreases from ~ 0.2 at low-iron sites to ~ 0.02 at high-iron sites. Varying phytoplankton communities and grazing pressure appear to explain this negative relationship. Our work emphasizes the need to consider detailed plankton community structure to

accurately identify the controls on carbon export efficiency, which appear to include small spatio-temporal variations of ecosystem structure.

1 Introduction

Physical and biological processes occuring in the surface ocean generate a vast diversity of particles. These particles represent potential vehicles to export organic carbon to the deep ocean where a small fraction can eventually be sequestered in the sediments. This process, known as the "biological carbon pump" (BCP) influences the level of atmospheric carbon dioxide and thus the global climate system (Volk and Hoffert, 1985; Lam et al., 2011).

Primary production in the euphotic layer builds a stock of phytoplankton cells. If their concentration and stickiness are high enough (Jackson, 1990), these can collide, attach and form large phytodetrital aggregates (Burd and Jackson, 2009; McCave, 1984); with those reaching sizes greater than 0.5 mm known as "marine snow" (Alldredge and Silver, 1988). Alternatively, phytoplankton cells can be tightly packed into dense fecal pellets through zooplankton grazing (Silver and Gowing, 1991). Because of their large size and high density respectively, phytodetrital aggregates and fecal pellets are major constituents of the downward flux, and several studies have found either fecal pellets (Fowler and Knauer, 1986; Pilskaln and Honjo, 1987; Bishop et al., 1977; Wassmann et al., 2000; Ebersbach and Trull, 2008; Cavagna et al., 2013) or large organic aggregates (Turner, 2002; Alldredge and Gotschalk, 1989; De La Rocha and Passow, 2007; Jackson, 1990; Burd and Jackson, 2009), to be the dominant vectors of carbon to depth.

Because grazing causes losses of organic carbon by respiration (Michaels and Silver, 1988; Alldredge and Jackson, 1995), direct export via the sinking of phytodetrital aggregates represents the most efficient operating mode of the BCP. However, ecosystem structure and environmental conditions under which primary production can be exported directly via phytodetrital aggregates are yet unclear and their determination would considerably improve the predictions of the efficiency of the BCP in varying conditions. The volume fraction of phytodetrital aggregates vs. fecal pellets in the total flux and their volume to carbon

content ratio, select the dominant carbon export mode; these relative contributions depend on numerous parameters including primary productivity, biomass, interactions between primary producers and heterotrophic communities (Michaels and Silver, 1988), physical fragmentation, microbial decomposition, coprophagy and the velocity at which particles settle (Turner, 2002).

The Southern Ocean contains the largest High Nutrient Low Chlorophyll (HNLC) area of the world ocean and is an essential player in global biogeochemistry (Sigman and Boyle, 2000). In these waters, abundant macronutrients (silicic acid, nitrate and phosphate) can fuel primary production given available light and sufficient iron, a limiting micronutrient (de Baar et al., 1995; Martin, 1990). The Kerguelen plateau offers the opportunity to study the functioning of the BCP in a naturally iron-fertilised region (Blain et al., 2007). The first KErguelen Ocean and Plateau compared Study (KEOPS1), demonstrated that most of the sinking flux collected in polyacrylamide gel sediment traps was derived from copepod fecal detritus (intact or degrading pellets and fecal ~~aggregates)~~ material reaggregated with phytodetritus, hereafter called "fecal aggregates"), and reported limited evidence for phytodetrital aggregates formed by direct flocculation of phytoplankton cells (Ebersbach and Trull, 2008). Number and volume fluxes were dominated by aggregates but they represented a small fraction of the total carbon flux, owing to their low volume to carbon content ratio. Several natural and artificial iron-fertilization experiments conducted at the same time of the year but in different locations in the Southern Ocean (e.g. SAZ-sense study and SOFeX), displayed similar export modes relying mainly on fecal matter (Bowie et al., 2011; Ebersbach et al., 2011; Coale et al., 2004; Lam and Bishop, 2007). In contrast, other artificial and natural iron experiments (SOIREE, CROZEX and EiFeX) have demonstrated a direct export via the sinking of phytodetrital aggregates or single phytoplankton cells (Boyd et al., 2000; Waite and Nodder, 2001; Pollard et al., 2007; Salter et al., 2007; Smetacek et al., 2012).

These variations among studies may reflect the time-varying aspects of export. In his review of Southern Ocean ecosystem contribution to carbon export, Queguiner (2013) suggests that from the onset of a bloom to its decline and subsequent export event, phytoplank-

ton, and to a lesser extent zooplankton communities, are subject to several rapid successions. The complexity of the processes is also reflected by the past 30 years of empirical and modelling studies attempting to relate deep carbon export variations to surface productivity (Eppley and Peterson, 1979; Suess, 1980; Wassmann, 1990; Guidi et al., 2009). In general, the ratio between export and production in the surface ocean is low ($<$ 5–10 %; Buesseler, 1998), but decoupling associated with high export events (e.g. high latitude blooms), or even negative relationships have been noted (Maiti et al., 2013; Buesseler, 1998; Ebersbach et al., 2011; Lam and Bishop, 2007). This highlights the complexity of food web structure and its multiple controls on carbon export (Wassmann, 1998; Michaels and Silver, 1988).

In the present study we test the hypothesis that direct export via phytodetrital aggregates occurs during the early stage of the Kerguelen naturally iron-fertilized bloom, when zooplankton communities present in the water column are not fully developed. We further explore the relative export abilities of each carbon export mode (i.e. phytodetrital aggregates vs. fecal pellets), by looking at their variation with depth and over time, and their links to spatio-temporal variations of plankton communities.

We collected sinking particles in free-drifting polyacrylamide gel and standard sediment traps. Gel traps allowed the collection of intact natural particles as they sank in the water column (Ebersbach and Trull, 2008; Jannasch et al., 1980; McDonnell and Buesseler, 2010), and thus gave a direct "picture" of the sinking flux at the depth of trap deployment. Image analysis of particles embedded in gels provided particle statistics (e.g. number and volume fraction of each category of particle), and conversion from area to volume and from volume to carbon content, using empirical relationships, allowed estimation of the carbon flux and the relative importance of each category of particle. In parallel, standard sediment traps serving as a reference, permitted direct quantitative estimates based on bulk chemical analyses of the material collected and from ^{234}Th depletion method (Planchon et al., 2014). Then, to test our main hypothesis, the relative contribution of each category of particles was linked to the amount of carbon effectively exported, to determine which one led the carbon export.

2 Material and methods

2.1 The KEOPS2 study

The second KErguelen Ocean and Plateau compared Study (KEOPS2) was conducted onboard the R.V. *Marion Dufresne* over and downstream of the Kerguelen plateau, from the 8 October to the 30 November 2011 (as described in detail in Blain, 2014). Sinking particle flux and composition were assessed by the use of free-drifting sediment traps deployed at six stations, inside and outside the naturally iron-fertilised area, in waters with varying biomass and surface chlorophyll *a* (Chl. *a*) levels (Fig. 1 ~~).~~ and 2). For more information on the complex spatio-temporal evolution of the phytoplankton bloom over the full 2011-2012 annual cycle, we refer the reader to an animation of NASA MODIS Aqua chlorophyll images, provided as a supplementary material in Trull et al. (2014). Combination of sediment trap collection with volume to carbon conversion factors allowed to determine preferential modes of carbon export (Ebersbach and Trull, 2008; Ebersbach et al., 2011).

2.2 Water column properties and biomass at each station

In addition to trap-derived measurements, POC concentrations were estimated in the water column using a WET Labs C-Star (6000 m) transmissometer (660 nm wavelength and 25 cm path length), linked to a conductivity-temperature-depth (CTD) system (Seabird SBE-911+CTD). Xmiss transmissometer data (%) were converted to POC concentrations ($\mu mol\,L^{-1}$), following a calibration based on in situ POC measurements from Niskin bottles. A Seapoint Chelsea Aquatracka III (6000 m) chlorophyll fluoremeter linked to the CTD was used to determine fluorescence profiles. Fluorescence was converted to chlorophyll *a* (Chl *a*; $\mu g\,L^{-1}$), by comparison with total Chl *a* in situ measurements from Niskin bottles (Lasbleiz et al., 2014).

Figure 2 shows water column properties and biomass at each site. The HNLC reference station R-2 located outside the fertilised area was characterised by a relatively deep mixed layer (96 m), low net primary productivity (euphotic zone 1 % PAR integrated NPP

$= 135 \pm 6\,\mathrm{mg\,C\,m^{-2}\,d^{-1}}$; Cavagna et al., 2014), low surface chlorophyll (chlorophyll *a* mixed layer average $= 0.6\,\mu\mathrm{g\,Chl\,}a\,\mathrm{L^{-1}}$), and biomass (mixed layer integrated POC $= 4.7\,\mathrm{g\,C\,m^{-2}}$). Stations E-1, E-3 and E-5 were located in an eddy-like, bathymetrically trapped recirculation feature in deep waters east of the Kerguelen islands (stationary meander of the polar front), with a mixed layer depth varying from 33 m (E-3) to 70 m (E-1). These stations had moderate NPP (523 ± 55, 686 ± 97 and $943 \pm 113\,\mathrm{mg\,C\,m^{-2}\,d^{-1}}$ respectively), chlorophyll *a* (0.8, 0.7 and 1.1 µ g Chl a $\mathrm{L^{-1}}$ respectively), and biomass (5.3, 3 and $4.8\,\mathrm{g\,C\,m^{-2}}$ respectively). They were used as a time series assuming a pseudo-lagrangian evolution (d'Ovidio et al., 2014). F-L was the only station located north of the polar front and exhibited the shallowest mixed layer (31 m). A3-2 was the second visit to the on-plateau bloom reference station of KEOPS1 and had the deepest mixed layer (149 m). F-L and A3-2 displayed the highest NPP (3.4 ± 0.1 and $1.9 \pm 0.2\,\mathrm{g\,C\,m^{-2}\,d^{-1}}$ respectively), chlorophyll *a* (3 and 1.8 µg Chl *a* $\mathrm{L^{-1}}$ respectively) and biomass (6.2 and $20.4\,\mathrm{g\,C\,m^{-2}}$).

2.3 Sediment trap preparation, deployments and recovery

Two different types of trap were deployed during KEOPS2. Bulk fluxes of particulate organic carbon (POC), total particulate nitrogen (TPN), biogenic silica (BSi), particulate inorganic carbon (PIC), particulate iron (PFe; data shown in Bowie et al., 2014) and thorium 234 (^{234}Th) were estimated using PPS3/3 traps (Technicap, La Turbie, France). A PPS3/3 trap consists of a single cylindrical trap with an internal conical funnel at its base with a collection area of $0.125\,\mathrm{m^2}$ that collects samples into a carousel of 12 cups. During KEOPS2, these traps were deployed for a maximum period of 6 days. Cups were filled with brine with a salinity of $\sim$ 52 psu, made by freezing filtered (0.2 µm pore size) surface seawater. Some cups were also amended with mercuric chloride ($1\,\mathrm{g\,L^{-1}}$) as a biocide (as detailed in Table 4). No poison was added to the cups used for trace metal studies (Bowie et al., 2014).

To examine sinking flux characteristics (particle type, number and size), intact particles were also collected in cylindrical polyacrylamide gel-filled sediment traps with a collection area of $0.011\,\mathrm{m^2}$. These deployments lasted less than two days to not overload the gels (Ta-

ble 1). Polyacrylamide gels were prepared following the method developed by Lundsgaard (1995), modified as described in Ebersbach and Trull (2008).

~~Each~~ Due to different required deployment durations (shorter for gel traps to avoid overloading, see above), each category of trap was deployed on separate arrays, except at A3-2 (combined deployment; Table 1). All separated deployments of gel and PPS3/3 traps overlapped in time and location (except at station E-3 where they were successive), to maximise the collection of similar particle fields. The arrays had broadly the same design consisting of a surface float sustaining a mooring line where the traps were fixed at different depths. PPS3/3 traps were fixed at 210 m and one to four gel traps, depending on the station, were fixed at 110, 210, 330 and 430 m. Wave-induced motions were dampened by an elastic to keep the traps at a constant depth (Trull et al., 2008). Pressure sensors mounted on the deepest gel trap and PPS3/3 trap on most of the arrays confirmed very small vertical motions during the deployments with depth standard deviations ranging from 0.6 m at E-1 to 2.4 m at E-5 (Table 1). The average trap drift speed of $8.5 \pm 5\,\mathrm{cm\,s^{-1}}$ was in the range of horizontal velocities determined by drogued drifter trajectories (Zhou et al., 2014). Inclinometers recorded little tilts of the mooring lines (from $0.3 \pm 1^\circ$ at E-3 to a maximum of $4 \pm 1.7^\circ$ at E-5), guaranteeing minimum perturbation of particle collection due to hydrodynamic conditions. No particular difficulties were encountered during trap recoveries, ensuring unperturbed gel structure. The seawater overlying the gels was removed directly after recovery to prevent particles collected in the trap cylinder during the recovery from entering the gels. Unfortunately, the PPS3/3 trap array deployed at R-2 was lost.

2.4 Chemical analysis

Protocols used for particulate organic carbon (POC), total particulate nitrogen (TPN), particulate inorganic carbon (PIC) and biogenic silica (BSi) analyses are described in Trull et al. (2008). ^{234}Th flux analysis is detailed in Planchon et al. (2014).

2.5 Image analysis

Within a few hours after recovery, each gel was photographed onboard against a laser etched-glass grid of 36 cells (each 14 mm $\times$ 12.5 mm) at a magnification of $\times$ 6.5 using a light field transmitted illumination and a Zeiss Stemi 2000-CS stereomicroscope coupled to a Leica DFC-280 1.5 million pixel digital camera and Leica Firecam software on an Apple iMac G4 computer. Observations at higher magnification (from $\times$ 10 to $\times$ 50) confirmed particle identifications when needed.

Pictures of incomplete grid cells, with inequally distributed particles or large zooplankton were removed from the analysis to avoid bias. Ten grid cells per gel (total of 180 pictures) were selected randomly. The average sum of the surface analysed per gel was $15.7 \pm 0.7\,cm^2$ corresponding to 14.3 ± 0.7 % of the trap collection area.

Particles collected in gels (Fig. 3) were phytodetrital aggregates (PA), cylindrical fecal pellets (CFP), oval fecal pellets, fecal aggregates (FA) and diatoms in the form of chains (e.g. the pennate *Fragilariopsis* spp.) or single cells (e.g. the centric *Thalassiosira* spp.). A ~~few zooplankton~~ few mesozooplankton specimens were collected (less than 10 ~~by~~ per gel), and were mostly represented by copepods (adult and copepodite stages), ~~appendicularians, foraminifera and radiolarians~~ and appendicularians. Foraminifera and radiolarians were also occasionally observed. Phytodetrital aggregates were loose and green, while fecal aggregates contained dense brown material. Most cylindrical fecal pellets had sharp edges and relatively constant diameters but some were tapered along their length and had blurred edges composed of unpacked fecal material or attached phytodetritus (Fig. 3B).

A preliminary image analysis ~~permitted to classify the particles in~~ was conducted to select the best analysis method in term of particle identification. Particles were classified into three main categories, based on their significant contribution to the flux: phytodetrital aggregates, cylindrical fecal pellets and fecal aggregates. ~~Fecal aggregates were distinguished from phytodetrital aggregates by their inclusions of dense fecal matter.~~ A fourth category, oval fecal pellets, was rare (less than one pellet per image in total), and its contribution to the flux was assumed negligible. ~~Particle characteristics were then determined by conversion~~

Pictures were converted to binary images, with threshold levels adjusted manually on each picture to ensure a minimum alteration of particle areas. The average alteration of particle area estimated on a subsample was an increase of 21.6 ± 7 % ($n = 169$) for particles having irregular shapes (e.g. aggregates *sensu lato* including phytodetrital and fecal aggregates), and an increase of 11.6 ± 7 % ($n = 44$) for cylindrical fecal pellets. Cylindrical fecal pellet and aggregate areas were systematically corrected for this overestimation.

Pictures were analysed with the US National Institutes of Health free software Image J. Typical shapes of each category of particle was determined manually on a subsample of particles. Matlab routines using specific sets of shape descriptors were then applied to all images to identify and separate each category of particle. Because fecal and phytodetrital aggregates had similar complex shapes, ~~fecal aggregates were~~ automated routines could not separate these particles efficiently. All fecal material was thus isolated manually from ~~phytodetrital aggregates,~~ all other particles based on the assumption that fecal matter is brown and denser than biologically unprocessed phytoplankton (Ebersbach et ~~-~~al., 2011). ~~Tests~~ From the resulting set of pictures, fecal aggregates were separated easily from cylindrical fecal pellets due to their very contrasted shapes. Tests on the efficiency of our automated selection, conducted on a ~~large sample~~large sample, showed that 93.4 % ($n = 397$) of cylindrical fecal pellets and 67.2 % ($n = 171$) of fecal aggregates were correctly identified by the set of shape descriptors chosen.

All particle characteristics investigated in this study and their units are reported in Table 2. An area cut off applied at 0.004 mm^2 (0.07 mm equivalent spherical diameter) removed all "fake particles" deriving from small gel imperfections and glass-grid or microscope lens cleanliness. This cut off removed 38 % of the total number of particles (mostly spurious particles and small single cells), but represented only a loss of 5.2 % of the total area of particles in the images, introducing a negligible bias.

Aggregate area was converted to equivalent spherical diameter (ESD) assuming spherical shape, and the volume was calculated from the ESD. Because cylindrical fecal pellets were not always straight, their volume ~~was~~ could not be accurately measured directly from their length and was calculated from their perimeter and area (independent from pellet

curvature), assuming a cylinder. The radius r of the cylinder section was determined by finding the minimum root of the polynomial:

$$4r^2 - Pr + A = 0 \quad (1)$$

where P is the perimeter and A is the projected area of the aggregate. The length L was calculated from the projected area and radius using the formula:

$$L = A/2r \quad (2)$$

The volume was then calculated from the radius and length.

The conversion from volume to carbon content was done by using different ratios and relationships depending on the particle considered. Figure 4 shows the relationship between carbon content and particle volume for different algorithms from the literature and those selected in this study. Based on values published by González and Smetacek (1994), the volume of cylindrical fecal pellets was converted to their organic carbon content using a ratio of 0.036 mg C mm^{-3} (Fig. 4, Line 2), as an average value for ~~copepod (~~copepod (Fig. 4, Line 1), and euphausiid fecal pellets (Fig. 4, Line 3). For fecal aggregates, we used the power relationship between POC content and aggregate volume V, POC (µg) $= 1.05V(\text{mm}^3)^{0.51}$, based on the fractal decrease of carbon content with size and determined empirically by Alldredge (1998) for fecal marine snow (Fig. 4, Line 4). The volume of phytodetrital aggregates was converted to carbon content using also a power relationship determined by Alldredge (1998) for diatom marine snow, POC (µg) $= 0.97V(\text{mm}^3)^{0.56}$ (Fig. 4, Line 5), assuming aggregates composed of phytoplankton not biologically processed. In contrast to Ebersbach and Trull (2008; Fig. 4, Line 6), very small particles (large single cells and aggregates composed of few cells~~and large single cells~~) were included in the category of phytodetrital aggregates and their volume to carbon conversion was done using the same relationship (Fig. 4, Line 5).

Particle number and volume fluxes are presented in the Sect. 3 as a function of size spectra. All particles were binned in 10 size classes spaced logarithmically to give the best representation of the whole size range (Jackson et al., 1997, 2005). To avoid bias, bins

containing 5 or fewer particles were not included in the ~~analysis~~flux spectrum analyses, as recommended by Jackson et al. (2005). ~~All particle characteristics investigated in this study and their units are reported in Table 2.~~

3 Results

3.1 Particles collected in polyacrylamide gel-filled sediment traps

3.1.1 Particle number, projected area and volume fluxes

Despite variations of deployment duration among sites exceeding 80 % (between 0.9 and 5.3 days; Table 1), an observation of raw images (Fig. 5) gives a broad preliminary indication on flux differences in term of particle abundance (e.g. low fluxes at R-2 and F-L, and higher at E-stations and A3-2). The lowest particle numbers, projected particle area and volume fluxes were collected at R-2 and F-L (Table 3 and Fig. 6), with particle volume fluxes of 2.5 ± 1 and $3 \pm 0.7\,\mathrm{cm^3\,m^{-2}\,d^{-1}}$ at R-2 and F-L respectively (all depths averaged). In contrast high fluxes were collected at E-stations with an average volume flux of $7.5 \pm 3\,\mathrm{cm^3\,m^{-2}\,d^{-1}}$ (all E-stations and depths averaged). Station A3-2 presented also a relatively high flux of $6.1\,\mathrm{cm^3\,m^{-2}\,d^{-1}}$.

Phytodetrital aggregates dominated in number at most stations and depths (49 ± 10 % of the total number of particles for all stations and depths averaged). Particles not selected automatically as phytodetrital aggregates, cylindrical fecal pellets or fecal aggregates ("others" on Table 3), represented the second largest numerical fraction (38 ± 8 %) but less than 9 % of the total projected particle area, and thus were assumed negligible in volume fluxes. Phytodetrital aggregates dominated also the volume fluxes (45.3 ± 22 %; all stations and depths averaged), with a maximum of 70 % at A3-2. However, volumes of cylindrical fecal pellets collected at E-5 (44 ± 33 %; all depths averaged) and volumes of fecal aggregates collected at F-L (57 ± 18 %; all depths averaged) represented the highest fractions at these stations.

Projected area fluxes at all stations and depths (Fig. 6), showed a clear attenuation of the total flux between 210 and 430 m (loss of 38 ± 21 % in average) with a maximum attenuation of 74 % at E-5 (Fig. 6a). A decrease of the flux of cylindrical fecal pellets with depth was combined with an increase of the flux of aggregates (mainly phytodetrital), except at R-2 where a general flux attenuation was observed (all particle categories), and only a small increase of phytodetrital aggregates at 430 m.

Fluxes at E-stations at 110 and 210 m decreased with time between E-1 and E-3, followed by a strong increase of cylindrical fecal pellet flux at E-5 (Fig. 6c).

3.1.2 Number and volume flux spectra

Smallest particles were the most numerous at every site and depth (Fig. 7). Particle numbers decreased more than three orders of magnitude for a one order of magnitude increase in size (0.008 to 0.07 cm), leading to slopes values around -3, so in the range expected for particle size distribution (PSD) in natural waters (-2 to -5; Buonassissi and Dierssen, 2010; Guidi et al., 2009) Phytodetrital aggregates, representing the largest fraction of total particles, followed broadly the same spectra. Most cylindrical fecal pellets and fecal aggregates were middle-sized (ESD of 0.015–0.1 cm) with maximum abundances in the range 0.015–0.03 cm. E-5 presented the highest abundance of large fecal pellets (0.025 to 0.035 cm) with values exceeding 2×10^7 and 7×10^6 # m^{-2} d^{-1} cm^{-1} at 110 m and 210 m respectively.

At all sites, most of the volume flux of phytodetrital aggregates was carried by middle sized particles (ESD of 0.01–0.03 cm), due to the small contribution of large aggregates to the total number. Middle-sized and large cylindrical fecal pellets and fecal aggregates (ESD of 0.03–0.07 cm) carried most of the volume flux, but again the largest particles did not bring the highest contribution due to their rarity relative to smaller particles (except at R-2 where the the largest cylindrical fecal pellets and fecal aggregates contributed significantly to the volume flux).

The most notable change of the number flux spectra with depth was observed for middle-sized cylindrical fecal pellets at E-stations, for which a decrease in number was generally

combined with an increase in size. E-1 presents the best illustration with most of cylindrical fecal pellets with a size around 0.01 cm at 110 m increasing to 0.06 cm at 210 m.

3.1.3 POC flux from image analysis

The lowest carbon fluxes were estimated at R-2 and F-L (Table 3), with values of 27 ± 12 and $36 \pm 10\,\mathrm{mg\,C\,m^{-2}\,d^{-1}}$ respectively (all depths averaged). The highest carbon fluxes were observed at E-stations ($107 \pm 33\,\mathrm{mg\,C\,m^{-2}\,d^{-1}}$, all E-stations and depths averaged) with a maximum value of $180\,\mathrm{mg\,C\,m^{-2}\,d^{-1}}$ at E-5, 110 m. A3-2 presented a moderate carbon flux of $66\,\mathrm{mg\,C\,m^{-2}\,d^{-1}}$ at 210 m.

Cylindrical fecal pellets carried most of the carbon flux at all stations and depths, with an average fractional contribution of 56 ± 19 % (Table 3). This was particularly true at E-stations where fecal pellets drove on average 63 ± 17 % of the carbon flux (maximum of 88 % at E-5, 110 m) and at F-L (62 ± 20 %, all depths averaged). However, at several stations, a transition was observed at 430 m where phytodetrital aggregates brought the largest fractional contribution with 63, 47 and 55 % at R-2, E-1 and E-5 respectively. Fecal aggregates carried generally a small fraction of the carbon flux with an average of 13 ± 8 % (all stations and depths), but their contribution tended to increase with depth (e.g. 24 % and 33 % at 430 m at R-2 and F-L respectively).

3.2 Biogeochemical fluxes collected in PPS3/3 traps

Bulk fluxes from PPS3/3 traps are reported in Table 4. The highest mass, POC, ^{234}Th and TPN fluxes were collected at E-stations. POC fluxes decreased over time from 84 ± 27 at E-1, to 58 ± 18 at E-3, and 24 ± 12 at E-5 $\mathrm{mg\,C\,m^{-2}\,d^{-1}}$. A3-2 presented a POC flux of $27\,\mathrm{mg\,C\,m^{-2}\,d^{-1}}$. An average ^{234}Th activity of $988 \pm 127\,\mathrm{dpm\,m^{-2}\,d^{-1}}$ was recorded at E-stations with a maximum of $1129 \pm 177\,\mathrm{dpm\,m^{-2}\,d^{-1}}$ at E-3. ^{234}Th fluxes are detailed in Planchon et al. (2014). Over all sites, BSi fluxes were very high (7 ± 2 to 21 ± 10 mmol BSi $\mathrm{m^{-2}\,d^{-1}}$), suggesting the large contribution of diatoms to the phytoplankton community. Conversely, very low particulate inorganic carbon (PIC) fluxes (3 to 4 orders of magnitude

lower than POC fluxes) suggested the limited role of calcium carbonate ($CaCO_3$) in biogenic mineral fluxes. POC : TPN ratios were close to the canonical Redfield ratio of 6.6 for phytoplankton, at all stations except E-5 (7.5) which also displayed the lowest POC : BSi ratio (0.1). At E-stations POC : ^{234}Th and POC : mass ratios decreased over time (POC : ^{234}Th ratios from 8 at E-1 to 2.1 µmol dpm^{-1} at E-5; POC : mass ratio from 0.05 at E-1 to 0.03 g g^{-1} at E-5), suggesting an attenuation of export fluxes combined with a degradation of sinking particles. A3-2 displayed POC : ^{234}Th and POC : mass ratios of 4.4 µmol dpm^{-1} and 0.06 g g^{-1} respectively. In general, no consistent differences in fluxes could be resolved between poisoned and unpoisoned cups.

3.3 POC flux comparisons and export efficiencies

POC fluxes determined from gel images (using particle volume to carbon content conversion factors) were in the same range of values as those determined from particle collection in PPS3/3 with maximum differences at a same station never exceeding one order of magnitude (Tables 3 and 4). POC fluxes from PPS3/3 were systematically lower than those derived from image analysis (in average 57 ± 22 % less).

E-ratios calculated as the ratio of POC fluxes from gel image analysis to 1 % PAR integrated net primary productivity (Cavagna et al., 2014; Table 5), indicated a high export efficiency at R-2 and E-1 (0.2 ± 0.08 and 0.23 ± 0.07 respectively, all depths averaged), intermediate at E-3 and E-5 (0.1 ± 0.02 and 0.13 ± 0.09 respectively, all depths averaged), and very low at F-L (0.01 ± 0.0, similar value at all depths) and A3-2 (0.03). E-ratios derived from POC fluxes estimated from PPS3/3 traps showed lower values but following the same trend: E-1 $>$ E-3 $>$ E-5 $>$ A3-2. Export efficiencies derived from ^{234}Th disequilibria, ThE_C (Planchon et al., 2014), are shown in Table 5 for comparison, and are discussed in the next section.

According to calculations based on gel trap POC flux and transmissometer POC concentration estimates (Fig. 2), E-stations exported the largest percentage of their mixed layer-integrated POC (ΣPOC_{ML}) per day (2.4 ± 1 %, all E-stations and depths averaged) with the maximum observed at E-5 (2.7 ± 1.8 %, all depths averaged) and values of 2.3 ± 0.7 % and

2.3 ± 0.5 % at E-1 and E-3 respectively (all depths averaged). R-2 and F-L exported respectively 0.58 ± 0.2 % and 0.59 ± 0.15 % of their ΣPOC_{ML} per day (all depths averaged), and A3-2 exported 0.32 % of its ΣPOC_{ML} per day (210 m). A similar trend was obtained using POC fluxes from PPS3/3 traps (E-stations $>$ A3-2).

4 Discussion

4.1 Comparison of POC flux estimations

Two different approaches were used to estimate POC fluxes. PPS3/3 trap collection providing a direct determination of the flux, served as a reference method. POC fluxes estimated from image analysis of particles embedded in polyacrylamide gels were in the same range than those derived from PPS3/3, but systematically higher (see Sect. 3). This difference is most likely due to the uncertainty on the volume to carbon conversion factors (Fig. 4), used to estimate POC fluxes from particle image analysis. A comparison with the direct estimation of bulk fluxes collected in PPS3/3 suggests that our volume to carbon content conversion factors tended to slightly overestimate the carbon carried by sinking particles (Tables 3 and 4), especially at E-5 where it was up to 7 fold higher. At this station the large contribution of cylindrical fecal pellets to the volume flux (Table 3; 72 % at 110 m and 51 % at 210 m) suggests that the volume to carbon conversion factor used for these particles may be responsible for the mismatch observed. The value of 0.036 mg C mm^{-3} used as an average for copepod and euphausiid fecal pellets may not reflect the actual carbon contained in the cylindrical fecal pellets collected. Feeding behaviours (e.g. herbivorous or coprophagous), specific to each zooplankton group will produce fecal pellets with variable carbon content due to variable fraction of undigested food, compaction or vulnerability to physical or biological degradation (Urban-Rich et al., 1998). Constant carbon to volume ratios are thus unable to reflect the myriad of fecal pellet compositions linked to ecosystem structure variations. Values of carbon content in cylindrical fecal pellets found in the literature range over approximately one order of magnitude between 0.01 and 0.1 mg C mm^{-3} (González and Smetacek,

1994; González et al., 1994, 2000; Carroll et al., 1998), leading to potential strong variations in carbon flux estimations if large volumes of fecal pellets are involved as it was the case at E-5. Mesozooplankton community collected in Bongo nets from 250 m to the surface (day and night haulings except at R-2 and F-L where only day haulings were conducted), and analysed with a ZooScan integrated system (Carlotti, 2014), revealed generally a large dominance of the size fraction 500–1000 µm with values from 54 to 79 % (considering only the stations where the traps were deployed). Microscopic identifications confirmed a community largely dominated by copepods (Carlotti, 2014). However, most of the fecal pellets collected in gel traps at E-5 were large fragments (Fig. 5), with a peritrophic membrane interrupted at their extremities suggesting more probably an origin from euphausiids rather than copepods which produce smaller fecal pellets with a continuous peritrophic membrane terminated by a pellicle (Gauld, 1957; Martens, 1978; Yoon et al., 2001). Differences in euphausiid and copepod fecal pellet sinking velocities due to size variations, ballast content or compaction (Fowler and Small, 1972; Small et al., 1979), and contrasted sensitivities to degradation or zooplankton vertical migration behaviours (Wallace et al., 2013), could explain the mismatch between the zooplankton community identified from net haulings and the fecal pellets collected in gel traps. A reduced collection efficiency of euphausiids compared to copepods could also be responsible for this mismatch, knowing that specific nets like the Multiple Opening and Closing Nets and Environment Sensing System (MOCNESS; Wiebe et al., 1976), are needed to capture efficiently both mesozooplankton and euphausiids in the layer 0–250 m (e.g. Espinasse et al., 2012). Most studies show that zooplankton net avoidance is complex and variable; it depends on environmental conditions (e.g. light regime), net characteristics and various zooplankton characteristics including size, shape, species, sex or developmental stage (Brinton, 1967; Fleminger and Clutter, 1965; Wiebe et al., 1982).

Assuming a dominance of ~~euphausiids~~ euphausiid fecal pellets at E-5, the use of the reference value of 0.016 $\mathrm{mg\,C\,mm^{-3}}$ improves the match between POC fluxes estimated from PPS3/3 and gel traps (ratios $\mathrm{POC_{gels}/POC_{PPS3/3}} = 4$), although it cannot fully explain

the discrepancy, presumably due to other factors (e.g. particle field heterogeneity or small differences in sediment trap collection efficiencies).

4.2 Evolution of the flux at depth

POC fluxes presented on Fig. 8, were estimated through two different approaches: gel trap image analysis (at 110, 210, 330 and 430 m), and total ^{234}Th activity measured at 11 to 14 depths at all stations (Planchon et al., 2014), and calculated at 100, 150 and 200 m. Fluxes estimated from PPS3/3 trap collection at only one depth (210 m) are not presented here. Figure 8 shows the evolution of POC fluxes with depth and its comparison with the empirical flux attenuation known as the "Martin curve" (Martin et al., 1987), estimating the flux at depth from values at 100 m ranging from 20 to 500 mg C m^{-2} d^{-1}. Agreements between POC flux determination methods and this empirical relationship were the best for R-2 and F-L, showing a continuous attenuation of the flux with depth, but always at a lower rate than predicted by the Martin curve.

For all other stations POC fluxes above 210 m presented complex patterns suggesting more likely distinct POC export episodes rather than a continuous downward flux. Between 210 and 430 m the attenuation of POC fluxes estimated from the gel traps tends to be more consistent with the Martin curve, except for E-5 which displayed a strong decrease (as already noted in the Sect. 3). A fecal pellet loss at depth was particularly strong at E-5, due to the large role played by these particles at this site, but was observed at all stations (Fig. 6).

Our data revealed two major trends of particle flux evolution with depth: (i) the fecal pellet flux decreased and (ii), phytodetrital and fecal aggregate fluxes remained constant or even increased. Establishing a link between these two processes is tempting. It suggests the importance of physical reaggregation in sustaining the carbon flux at depth from fecal pellets that have undergone bacterial degradation or zooplankton coprorhexy (Suzuki et al., 2003; Lampitt et al., 1990; Iversen and Poulsen, 2007). A recent study from Giering et al. (2014) suggests that half of fast-sinking particles in the twilight zone of the eastern Atlantic Ocean (between 50 and 1000 m), are fragmented and ingested by zooplankton, and that more than

30 % may be released as suspended and slowly sinking organic matter. Even if the gel trap technique does not offer enough information on aggregation processes and particle sources to permit any clear conclusion, the hypothesis of a reaggregation of unpacked fecal pellets into “secondary” phytodetrital aggregates still deserves careful consideration.

Since the rate of physical aggregation is largely controlled by particle concentration (Jackson, 1990), a reaggregation at depth implies that sufficient material has been released by fecal pellet disaggregation. If single cells represented most of the material released during fecal pellet disaggregation, their concentration should have increased with depth in the case of no secondary aggregation, or be constant as a balance between aggregate formation and loss by sinking (notion of critical concentration; Jackson, 1990, 2005). The number flux spectra (Fig. 7) suggests that the smallest particles had a constant concentration until 210 m at almost every site. Station E-3 shows an increase of the number of small particles between 110 and 210 m and then a decrease at 430 m, which could indicate reaggregation processes occuring at depth. This decrease at 430 m is also observable at E-5 and F-L. However, data evaluation in this way implies a steady state assumption which considers that traps measured the occurence of a unique sinking event; the flux collected at depth being a direct temporal evolution of the same shallower flux. This appears unlikely considering the episodic nature of export and its dependence on highly dynamical ecosystem interactions responsible for high flux variability at short spatio-temporal scales as evidenced by the PPS3/3 individual cup variations (Table 4). ~~A~~In addition, if assuming phytodetrital aggregates at E-3, sinking at an average velocity of 150 $\mathrm{m\,d^{-1}}$ (based on results from Laurenceau-Cornec et al., 2014), a particle field would need approximately 1.5 days to sink from 210 to 430 m, neglecting any advection. Considering this calculation and the short trap deployment at E-3 (1.02 days), a non steady state assumption appears more reasonable, and the increase of phytodetrital and fecal aggregates observed at depth could reflect an earlier production event.

4.3 Temporal POC flux variations during KEOPS2 and comparison with KEOPS1

From E-1 to E-5, the POC flux varied with the depth and estimation method. Collection of POC flux in PPS3/3 trap at 210 m revealed a monotonic decrease of the flux with time (Table 4). Temporal evolution of the flux between E-1, E-3 and E-5, at 100 ± 10 and 200 ± 10 m, using gel trap and ^{234}Th method (Planchon et al., 2014), shows a almost constant flux (undistinguishable differences within the uncertainties). At 430 m, gel traps measured flux evolutions comparable to those identified in the PPS3/3 at 210 m, i.e. a continuous decrease of the flux with time. Excluding the results from 110 and 210 m at E-5 (likely linked to an episodic flux of euphausiid fecal pellets at these depths, see text above), the gel traps show also a decrease of the total flux over time, consistent with PPS3/3 trap method. The unusual increase at E-5, against the steady background of the other E-stations, highlights the importance of zooplankton in modifying the particle flux.

At the KEOPS1 (January-February 2005) bloom reference station A3, POC flux values estimated at 200 m from gel trap image analysis and PPS3/3 traps, were 62 and 13–20 mg C m^{-2} d^{-1} respectively (Ebersbach and Trull, 2008), i.e. in the same range as during KEOPS2 at the same station and using the same methods (gels: 66 mg C m^{-2} d^{-1}; PPS3/3: 27 mg C m^{-2} d^{-1}). During KEOPS1, the ^{234}Th-based method assuming non steady statesystem (NSS) yielded 200 m-POC fluxes of 294 mg C m^{-2} d^{-1} at A3 (flux averaged over 21 days) and 124 mg C m^{-2} d^{-1} at the KEOPS1 HNLC reference station C11 (flux averaged over 10 days; Savoye et al., 2008). These values are well above the KEOPS2 values of 46 and 22 mg C m^{-2} d^{-1} determined at 200 m at A3-2 and R-2 respectively, using the same method (average over 28 days; except for R-2 assumed in steady state; Planchon et al., 2014). The ^{234}Th-based method assuming NSS, integrated the POC flux over a period longer than 20 days, contrasting with the one day to one week period provided by gel and PPS3/3 trap estimations.

Seasonal trends are more reliable if calculated over a longer period, and ^{234}Th-based method gives then the best insight into the temporal evolution of the POC flux from the on-

set of the bloom to its decline. ^{234}Th results suggest that the POC flux was approximately 5- to 6 fold higher at the decline of the bloom (January–February) than during its onset (October–November), agreeing with the common view that most of the export flux occurs in late bloom stage (Wassmann, 1998). During KEOPS1, at A3 and C11, the net primary productivity (NPP) integrated within the euphotic zone was 1030 ± 43 and 224 ± 30 mg C m^{-2} d^{-1} respectively (based on ^{13}C incorporation; Mosseri et al., 2008; Lefèvre et al., 2008). In comparison, values of 1903 ± 186 and 135 ± 6 mg C m^{-2} d^{-1} were determined at A3-2 and R-2 during KEOPS2 (euphotic zone, E_Z 1 % PAR integrated NPP based on ^{13}C incorporation; Cavagna et al., 2014). Carbon export efficiencies estimated at 200 m, based on ^{234}Th-derived POC export flux (reported as ThE_C) were 30 % at A3 and 49 % at C11 during KEOPS1 (calculations using data from Savoye et al., 2008; Mosseri et al., 2008). In contrast, ThE_C of 2 % (NSS model) and 16 % (SS model) were calculated at 200 m at A3-2 and R-2 respectively during KEOPS2 (Planchon et al., 2014). These results show that: (i) primary productivity at the on-plateau site was approximately 2 fold higher in spring than during summer, (ii) carbon export fluxes were approximately 5 fold lower during early than late bloom stage, leading to (iii), carbon export efficiencies up to 10 fold lower during the early (spring) than late bloom stage (summer).

4.4 Toward an explanation of the negative relationship between primary productivity and carbon export efficiency

We examined two different export efficiency indicators (Table 5): (i) e-ratios calculated as the ratio between POC fluxes estimated from gel images or PPS3/3 traps, and net primary productivity integrated over the euphotic zone (E_Z 1 % PAR; Cavagna et al., 2014), and (ii) ThE_C calculated as the ratio between POC flux estimated from ^{234}Th method and net primary productivity. KEOPS2 results suggest a negative relationship between primary productivity and carbon export efficiency, the most productive sites being those where carbon is exported the least efficiently. Figure 9a shows the relationship between primary productivity and export efficiency (with POC fluxes estimated at 200 ± 10 m from gels, PPS3/3 traps and ^{234}Th water column disequilibria) for KEOPS2 sites. For comparison purposes, KEOPS1

data are also indicated (Savoye et al., 2008). The empirical relationship proposed recently by Maiti et al. (2013), based on surface tethered cylindrical sediment traps and ^{234}Th data from up to 130 stations in the Southern Ocean is also reported. While this negative relationship has been observed now in several field studies in the Southern Ocean (Savoye et al., 2008; Morris et al., 2007; Jacquet et al., 2011), and elsewhere (e.g. González et al., 2009), the reasons for its existence remain unclear. As possible explanations of high productivity-low export efficiency regimes, Maiti et al. (2013) mentioned differences in trophic structure, grazing intensity, recycling efficiency, high bacterial activity, or increase in DOC export. Phytoplankton physiological state has also been suggested as a possible control of carbon export mode and efficiency (González et al., 2009), although this could not be verified here due to a general good phytoplankton physiological state confirmed via microscopy over the course of the KEOPS2 study (M. Lasbleiz and K. Leblanc, personal communication, 2014). In addition, due to their degradation-resistant and ~~heavily silicified~~ heavily-silicified valves (Hargraves and French, 1983; Kuwata and Takahashi, 1990), the abundance of diatom resting spores in the sinking flux, as observed during KEOPS1 (Armand et al., 2008), could also be a major factor to consider when evaluating carbon export efficiency as suggested by Salter et al. (2012) and Rynearson et al. (2013).

It was beyond the scope of this study to explore each of these potential controls of carbon export efficiency. However, in the light of KEOPS1 and KEOPS2 results, phytoplankton and zooplankton community structure and their trophic relationships through grazing, seem to have played an important role in carbon export mode and efficiency via controls on sinking particle composition.

Table 6 presents a summary of site characteristics based on net primary productivity, surface plankton communities determined from Niskin bottle sampling and net haulings (most abundant species and biomass), carbon export features at 200 ± 10 m (mode and efficiency) and iron fertilization status (e.g. HNLC or iron-fertilized). Due to their ~~apparent~~ importance in export fluxes demonstrated by high BSi fluxes (see Sect. 3), only diatoms were examined in the phytoplankton community. Data are presented for all stations but only

stations R-2 and A3-2 will be discussed ~~here~~ in detail here because of their reference status (i.e. HNLC and on-plateau bloom).

At the HNLC reference station R-2, characterised by the lowest net primary productivity (Cavagna et al., 2014), the diatom community was dominated by ~~the heavily silicified~~ the heavily-silicified *Fragilariopsis* spp. ~~and *Thalassionema nitzschioides* (~~(fraction of the whole diatom community: 34.6 %, M. Lasbleiz, personal communication, 2014) and *Thalassionema nitzschioides* (25.6 %), and by a limited mesozooplankton biomass represented mainly by middle-sized copepods (Carlotti et al., 2014). The export was mostly mediated through physical aggregation as suggested by the dominance of phytoplankton and fecal aggregates. The highest e-ratio estimated during KEOPS2 was observed at R-2. In contrast, the iron-fertilized on-plateau bloom station A3-2 displayed a high net primary productivity (Cavagna et al., 2014) and a diatom community largely dominated by the ~~slightly-silicified~~ lightly-silicified *Chaetoceros* subgenus *Hyalochaete* (~~M. Lasbleiz, personal communication, 2014~~87 %). The mesozooplankton biomass was ~~the lowest~~ high at A3-2. Small and middle-sized copepods dominated, along with euphausiid eggs and appendicularians (Carlotti, 2014). Particle exported were mostly phytodetrital aggregates. One of the lowest e-ratio was recorded at A3-2. At E-stations, used as a time series, the net primary productivity was moderate (Cavagna et al., 2014), and a shift from a high e-ratio at E-1 to a low e-ratio at E-5 was associated with plankton community shifts. This is indicated for instance by the remarkable increase of *Chaetoceros* subgenus *Hyalochaete* biomass from 10 and 2.3 % at E-1 and E-3 respectively to 22.5 % at E-5.

At ~~these two stations~~ stations R-2 and A3-2, although presenting very contrasted export efficiencies, physical aggregation seemed to dominate over biological aggregation, as suggested by the rarity of fecal pellets. If explained from this perspective, the inverse relationship between net primary productivity and export efficiency needs somewhat to be linked to the different nature of the aggregates produced at each station and their ability to export carbon to depth (e.g. slow- or fast-sinking). ~~Roller tank experiments consisting~~ In parallel of the present study, roller tank experiments have been conducted to explore the influence of different phytoplankton communities on the sinking velocity of large phytodetrital aggregates

and their aggregation processes (Laurenceau-Cornec et al., 2014). These experiments consisted in the physical aggregation of natural assemblages sampled with Niskin bottles at high and low biomass sites during KEOPS2~~, suggested that phytoplankton types could influence marine snow aggregate sinking velocities via a~~ . Results suggest that the proportions of different phytoplankton types forming the phytodetrital aggregates could influence their sinking velocity (and potentially their efficiency at exporting carbon), via a control on their structure and excess density~~(Laurenceau et al., 2014)~~. A strong relationship ($r^2 = 0.98$) was found between the proportion of small spine-forming diatom cells included in marine snow aggregates (e.g. *Chaetoceros* subgenus *Hyalochaete*), and their sinking velocity, suggesting an important role for phytoplankton morphology on export efficiency. However, no evidence has been made that natural phytoplankton communities present at each site as determined from Niskin bottle sampling (Table 6), reflect the composition of their aggregates, something required to approximate their sinking velocity from roller tank experiment results. Experimental and field studies noted that the proportions of diatoms in aggregates is not necessarily the same as their proportions in the surrounding water (Riebesell et al., 1991; Crocker and Passow, 1995; Waite and Nodder, 2001). Without direct estimation of the sinking velocity of natural aggregates formed in the water column at each station, no conclusion is possible and further investigations will be needed.

The potential control of export efficiency through zooplankton grazing is the other hypothesis that we explored here. In the case of high grazing pressure, carbon export is driven mostly via fecal pellets, but these, even if sinking fast, potentially experience coprophagy or coprorhexy (Suzuki et al., 2003; Lampitt et al., 1990; Iversen and Poulsen, 2007), and disaggregation processes facilitating bacterial remineralization (Giering et al., 2014). In Fig. 9b mesozooplankton biomass data from KEOPS2 (250 m to surface Bongo net haulings; Carlotti et al., 2014) is shown as a simple indice of zooplankton abundance against export efficiency. Considering all POC flux estimation methods, a correlation has been found ($n = 15$, $r^2 = 0.72$, $p < 0.0005$), suggesting that zooplankton may exert an important control on export efficiency. In this perspective, however, E-3 presented an unexpectedly high

export efficiency considering its high zooplankton biomass, suggesting that factors predominantly affecting carbon export efficiency can vary locally and over time.

In the ~~case of high grazing pressure, carbon export is driven mostly via fecal pellets, but these, even if sinking fast, potentially experience disaggregation processes, bacterial degradation and coprophagy or coprorhexy (Suzuki et al. , 2003; Lampitt et al. , 1990; Iversen and Poulsen, 2007). In the sites of high productivity (i. e. A3-2 and~~low productive systems (e.g. R-2), a direct export can be efficient if processed via fast-sinking aggregates composed of heavy-silicified diatoms that are also assumed to be grazing-resistant. In contrast, in the sites of high productivity (e.g. A3-2 and F-L), the export flux can be strongly attenuated if a large fraction of the organic carbon flows toward paths promoting its retention in the surface layer (i.e. grazing, microbial remineralization and biomass accumulation). At A3, Christaki et al. (2014), proposed a carbon budget integrated over the mixed layer showing the carbon flows through microbial and higher trophic levels for early and late bloom stages. This budget indicates that during KEOPS2, 2400 $mg\,C\,m^{-2}\,d^{-1}$ were still available for phytoplankton biomass accumulation and/or export, after substracting from the Gross Community Production (GCP), the different loss terms due to bacterial, other microplankton and mesozooplankton respiration and virus bacterial lysis. Using our carbon flux value at 200 m and phytodetrital aggregate contributions to this export, the relative fractions of the available carbon actually used for biomass accumulation and/or export can be estimated here. At A3-2, the carbon flux at 200 m was 66 $mg\,C\,m^{-2}\,d^{-1}$ (gel trap results), with 41 % contributed by phytodetrital aggregates (Table 3). This leads to 27 $mg\,C\,m^{-2}\,d^{-1}$ exported (1.1 % of the remaining available carbon) and 2373 $mg\,C\,m^{-2}\,d^{-1}$ used for biomass accumulation (98.9 %). The same calculations can be made for the late-bloom situation using the values of 384 $mg\,C\,m^{-2}\,d^{-1}$ for the carbon still available for biomass accumulation and/or export (Christaki et al., 2014), the ~~phytoplankton community might have been either unable to export carbon directly and efficiently because potentially producing slow-sinking aggregates~~KEOPS1 200 m POC flux at A3 (~~see discussion above) , or under a high grazing pressure where the zooplankton community was already well installed. In contrast, the low productive systems, like R-2,~~

~~presented a high export efficiency, possibly because export could have been direct via fast-sinking aggregates composed of heavy silicified diatoms that are also assumed to be grazing-resistant~~62 mg C m^{-2} d^{-1}; Ebersbach and Trull, 2008), and a 36 % aggregate contribution (including both phytodetrital and mixed aggregates; Ebersbach and Trull, 2008). Results lead to 22 mg C m^{-2} d^{-1} exported (5.7 %) and 362 mg C m^{-2} d^{-1} used for biomass accumulation (94.3 %). These estimations show that the fraction of the carbon available that is exported, is subjected to the largest variations during the season (increased by a factor of $\sim$5); while the fraction allocated to biomass accumulation varied comparatively much less (decreased by a factor of $\sim$1.05). It suggests that A3 progressed over the whole season from a retention- to an export-dominated food web system (Wassmann, 1998), possibly related to successions of plankton communities prone to large variations of their export ability, as suggested in this study.

This general picture can be compared with the conceptual scheme of the development of planktonic communities in the Southern Ocean, recently proposed by Queguiner (2013). Direct export can occur efficiently when the phytoplankton community is dominated by the large ~~heavily silicified~~ heavily-silicified species (e.g. *Fragilariopsis* spp.), which are highly grazing-resistant and form fast-sinking aggregates. This type of slow-growing species develops through the whole season and forms a "persistant" background encountered at almost all sites. In bloom conditions (during the growth season), smaller fast-growing ~~lightly silicified~~ lightly-silicified species are added to the community leading to an increased primary productivity. Because these small species are possibly less efficient at exporting carbon (e.g. rapidly grazed and/or sinking slowly), the increase in primary productivity is not accompanied by an increase in carbon export – though 2- to 5 fold higher in sites under Fe-fertilization influence than in HNLC site – required to obtain a high export efficiency.

5 Conclusions

To conclude, our study demonstrated that in early spring, during bloom initiation:

(i) Phytodetrital aggregates represented the main numerical and volume fractions of the flux, especially at depth, and could have played a major role in sustaining export fluxes where fecal pellet flux attenuation occured. This contrasts with summer time (KEOPS1), when fecal material dominated largely the flux while phytodetrital aggregates brought only a little contribution to the flux (Ebersbach and Trull, 2008). However, when converted to carbon content, and where their degradation was limited, cylindrical fecal pellets still represented the dominant fraction of the flux.

(ii) Primary productivity was negatively correlated to export efficiency, the highest productive sites being the least efficient to export carbon. This supports the emergent vision of high productivity low export regimes already noted in the Southern Ocean (Lam and Bishop, 2007). The decrease of productivity from bloom initiation (KEOPS2) to its decline (KEOPS1), related to a shift from ~~autotroph~~ autotroph- to heterotroph-dominated regimes (i.e. production exported via phytodetrital vs fecal material), could explain why major export tends to occur at the end of the season essentially via the sinking of fecal matter.

(iii) Plankton community structure influenced by productivity regimes, could have controlled export efficiency via variations in phytoplankton species and zooplankton grazing pressure ~~.~~ (Table 6).

Acknowledgements. This work received support from the Australian Commonwealth Cooperative Research Centres Program to the ACE CRC, and the Australian National Network in Marine Science via UTAS IMAS. We thank the personnel of the R.V. *Marion Dufresne*, Institut Paul Emile Victor, Institut National des Sciences de l'Univers, and the KEOPS2 voyage leader Bernard Queguiner and KEOPS2 science team for assistance at sea. Peter Jansen (IMOS), Danny McLaughlan (CSIRO) and David Cherry (CSIRO) contributed to prepare the free-drifting sediment trap arrays. MODIS (NASA) satellite ocean-colour images courtesy of Francesco d'Ovidio (Univ. Paris). The altimeter and colour/temperature products for the Kerguelen area were produced by Ssalto/Duacs and CLS with support from CNES.

References

Alldredge, A.: The carbon, nitrogen and mass content of marine snow as a function of aggregate size, Deep-Sea Res. Pt. I, 45, 529–541, doi:10.1016/S0967-0637(97)00048-4, 1998.

Alldredge, A. L. and Gotschalk, C. C.: Direct observations of the mass flocculation of diatom blooms: characteristics, settling velocities and formation of diatom aggregates, Deep-Sea Res., 36, 159–171, doi:10.1016/0198-0149(89)90131-3, 1989.

Alldredge, A. L. and Jackson, G. A.: Preface: aggregation in marine systems, Deep-Sea Res. Pt. II, 42, 1–7, doi:10.1016/0967-0645(95)90003-9, 1995.

Alldredge, A. L. and Silver, M. W.: Characteristics, dynamics and significance of marine snow, Prog. Oceanogr., 20, 41–82, doi:10.1016/0079-6611(88)90053-5, 1988.

Armand, L. K., Crosta, X., Queguiner, B., Mosseri, J., and Garcia, N.: Diatoms preserved in surface sediments of the northeastern Kerguelen Plateau, Deep-Sea Res. Pt. II, 55, 677–692, doi:10.1016/j.dsr2.2007.12.032, 2008.

Bishop, J. K. B., Edmond, J. M., Ketten, D. R., Bacon, M. P., and Silker, W. B.: The chemistry, biology, and vertical flux of particulate matter from the upper 400 m of the equatorial Atlantic Ocean, Deep Sea Research, 24, 511–548, doi:10.1016/0146-6291(77)90526-4, 1977.

Blain, S.: KEOPS2: implementation and overview, Biogeosciences Discuss., in preparation, 2014.

Blain, S., Queguiner, B., Armand, L., Belviso, S., Bombled, B., Bopp, L., Bowie, A., Brunet, C., Brussaard, C., Carlotti, F., Christaki, U., Corbiere, A., Durand, I., Ebersbach, F., Fuda, J. L., Garcia, N., Gerringa, L., Griffiths, B., Guigue, C., Guillerm, C., Jacquet, S., Jeandel, C., Laan, P., Lefevre, D., Lo Monaco, C., Malits, A., Mosseri, J., Obernosterer, I., Park, Y. H., Picheral, M., Pondaven, P., Remenyi, T., Sandroni, V., Sarthou, G., Savoye, N., Scouarnec, L., Souhaut, M., Thuiller, D., Timmermans, K., Trull, T., Uitz, J., van Beek, P., Veldhuis, M., Vincent, D., Viollier, E., Vong, L., and Wagener, T.: Effect of natural iron fertilization on carbon sequestration in the Southern Ocean, Nature, 446, 1070–1074, doi:10.1038/nature05700, 2007.

Bowie, A. R., Trull, T. W., and Dehairs, F.: Estimating the sensitivity of the subantarctic zone to environmental change: The SAZ-Sense project, Deep-Sea Res. Pt. II, 58, 2051–2058, doi:10.1016/j.dsr2.2011.05.034, 2011.

Bowie, A. R., van der Merwe, P., Trull, T. W., Quéroué, F., Fourquez, M., Planchon, F., Sarthou, G., and Blain, S.: Iron budgets for three distinct biogeochemical sites around the Kerguelen plateau (Southern Ocean) during the natural fertilization experiment KEOPS2, Biogeosciences Discuss., in preparation, 2014.

Boyd, P. W., Watson, A. J., Law, C. S., Abraham, E. R., Trull, T., Murdoch, R., Bakker, D. C. E., Bowie, A. R., Buesseler, K. O., and Chang, H.: A mesoscale phytoplankton bloom in the polar Southern Ocean stimulated by iron fertilization, Nature, 407, 695–702, doi:10.1038/35037500, 2000.

Brinton, E.: Vertical migration and avoidance capability of euphausiids in the California Current, Limnol. Oceanogr., 12, 451–483, doi:10.4319/lo.1967.12.3.0451, 1967.

Buesseler, K. O.: The decoupling of production and particulate export in the surface ocean, Global. Biogeochem. Cy., 12, 297–310, doi:10.1029/97GB03366, 1998.

Buesseler, K. O., Bacon, M. P., Kirk Cochran, J., and Livingston, H. D.: Carbon and nitrogen export during the JGOFS North Atlantic Bloom experiment estimated from $^{234}Th:^{238}U$ disequilibria, Deep-Sea Res., 39, 1115–1137, doi:10.1016/0198-0149(92)90060-7, 1992.

Buonassissi, C. and Dierssen, H.: A regional comparison of particle size distributions and the power law approximation in oceanic and estuarine surface waters, J. Geophys. Res., 115, C10028, doi:10.1029/2010JC006256, 2010.

Burd, A. B. and Jackson, G. A.: Particle aggregation, Annu. Rev. Mar. Sci., 1, 65–90, doi:10.1146/annurev.marine.010908.163904, 2009.

Carlotti, F.: Mesozooplankton structure and functioning during the onset of the Kerguelen Bloom during the KEOPS2 survey, Biogeosciences Discuss., in preparation, 2014.

Carroll, M. L., Miquel, J.-C., and Fowler, S. W.: Seasonal patterns and depth-specific trends of zooplankton fecal pellet fluxes in the Northwestern Mediterranean Sea, Deep-Sea Res. Pt. I, 45, 1303–1318, doi:10.1016/S0967-0637(98)00013-2, 1998.

Cavagna, A.-J., Dehairs, F., Bouillon, S., Woule-Ebongué, V., Planchon, F., Delille, B., and Bouloubassi, I.: Water column distribution and carbon isotopic signal of cholesterol, brassicasterol and particulate organic carbon in the Atlantic sector of the Southern Ocean, Biogeosciences, 10, 2787–2801, doi:10.5194/bg-10-2787-2013, 2013.

Cavagna, A.-J., Lefèvre, D., Dehairs, F., Elskens, M., Fripiat, F., Closset, I., Lasbleiz, M., Flores-Leive, L., Cardinal, D., Leblanc, K., Fernandez, C., Oriol, L., Blain, S., and Queguiner, B.: Biological productivity regime in the surface water around the Kerguelen Island in the Southern Ocean – from the use of an integrative approach, Biogeosciences Discuss., in preparation, 2014.

Christaki, U., Lefèvre, D., Georges, C., Colombet, J., Catala, P., Courties, C., Sime-Ngando, T., Blain, S., and Obernosterer, I.: Microbial food web dynamics during spring phytoplankton blooms in the naturally iron-fertilized Kerguelen area (Southern Ocean), Biogeosciences Discuss., 11, 6739–6753, doi:10.5194/bg-11-6739-2014, 2014.

Coale, K. H., Johnson, K. S., Chavez, F. P., Buesseler, K. O., Barber, R. T., Brzezinski, M. A., Cochlan, W. P., Millero, F. J., Falkowski, P. G., Bauer, J. E., Wanninkhof, R. H., Kudela, R. M., Altabet, M. A., Hales, B. E., Takahashi, T., Landry, M. R., Bidigare, R. R., Wang, X., Chase, Z., Strutton, P. G., Friederich, G. E., Gorbunov, M. Y., Lance, V. P., Hilting, A. K., Hiscock, M. R., Demarest, M., Hiscock, W. T., Sullivan, K. F., Tanner, S. J., Gordon, R. M., Hunter, C. N., Elrod, V. A., Fitzwater, S. E., Jones, J. L., Tozzi, S., Koblizek, M., Roberts, A. E., Herndon, J., Brewster, J., Ladizinsky, N., Smith, G., Cooper, D., Timothy, D., Brown, S. L., Selph, K. E., Sheridan, C. C., Twining, B. S., and Johnson, Z. I.: Southern Ocean iron enrichment experiment: carbon cycling in high- and low-Si waters, Science, 304, 408–414, doi:10.1126/science.1089778, 2004.

Crocker, K. M. and Passow, U.: Differential aggregation of diatoms, Mar. Ecol.-Prog. Ser., 117, 249–257, doi:10.3354/meps117249, 1995.

d'Ovidio, F.~~: Pathways of iron dispersion off the Kerguelen Plateau: the~~ , Della Penna, A., Trull, T. W., Nencioli, F., Pujol, I., Rio, M. H., Cotté, C., Zhou, M., and Blain, S.: The biogeochemical structuring role of horizontal stirring: Lagrangian perspectives on iron delivery downstream of the Kerguelen plateau, Biogeosciences Discuss., in preparation, 2014.

de Baar, H. J. W., de Jong, J. T. M., Bakker, D. C. E., Loscher, B. M., Veth, C., Bathmann, U., and Smetacek, V.: Importance of iron for plankton blooms and carbon dioxide drawdown in the Southern Ocean, Nature, 373, 412–415, doi:10.1038/373412a0, 1995.

De La Rocha, C. and Passow, U.: Factors influencing the sinking of POC and the efficiency of the biological carbon pump, Deep-Sea Res. Pt. II, 54, 639–658, doi:10.1016/j.dsr2.2007.01.004, 2007.

Ebersbach, F. and Trull, T. W.: Sinking particle properties from polyacrylamide gels during the KErguelen Ocean and Plateau compared study (KEOPS): Zooplankton control of carbon export in an area of persistent natural iron inputs in the Southern Ocean, Limnol. Oceanogr., 53, 212–224, doi:10.4319/lo.2008.53.1.0212, 2008.

Ebersbach, F., Trull, T. W., Davies, D. M., and Bray, S. G.: Controls on mesopelagic particle fluxes in the Sub-Antarctic and Polar Frontal Zones in the Southern Ocean south of Australia in summer – Perspectives from free-drifting sediment traps, Deep-Sea Res. Pt. II, 58, 2260–2276, doi:10.1016/j.dsr2.2011.05.025, 2011.

Eppley, R. W. and Peterson, B. J.: Particulate organic matter flux and planktonic new production in the deep ocean, Nature, 282, 677–680, doi:10.1038/282677a0, 1979.

Espinasse, B., Zhou, M., Zhu, Y., Hazen, E., Friedlaender, A., Nowacek, D., Chu, D., and Carlotti, F.: Austral fall–winter transition of mesozooplankton assemblages and krill aggregations in an embayment west of the Antarctic Peninsula, Mar. Ecol.-Prog. Ser., 452, 63–80, 2012.

Fleminger, A. and Clutter, R. I.: Avoidance of towed nets by zooplankton, Limnol. Oceanogr., 10, 96–104, doi:10.4319/lo.1965.10.1.0096, 1965.

Fowler, S. W. and Knauer, G. A.: Role of large particles in the transport of elements and organic compounds through the oceanic water column, Prog. Oceanogr., 16, 147–194, doi:10.1016/0079-6611(86)90032-7, 1986.

Fowler, S. W. and Small, L. F.: Sinking rates of euphausiid fecal pellets, Limnol. Oceanogr., 17, 293–296, doi:10.4319/lo.1972.17.2.0293, 1972.

Gauld, D. T.: A peritrophic membrane in calanoid copepods, Nature, 179, 325–326, doi:10.1038/179325a0, 1957.

Giering, S. L. C., Sanders, R., Lampitt, R. S., Anderson, T. R., Tamburini, C., Boutrif, M., Zubkov, M. V., Marsay, C. M., Henson, S. A., Saw, K., Cook, K., and Mayor, D. J.: Reconciliation of the carbon budget in the ocean's twilight zone, Nature, 507, 480–483, doi:10.1038/nature13123, 2014.

González, H. E. and Smetacek, V.: The possible role of the cyclopoid copepod *Oithona* in retarding vertical flux of zooplankton faecal material, Mar. Ecol.-Prog. Ser., 113, 233–246, doi:10.3354/meps113233, 1994.

González, H., González, S., and Brummer, G.: Short-term sedimentation pattern of zooplankton, faeces and microplankton at a permanent station in the Bjørnafjorden (Norway) during April–May 1992, Mar. Ecol.-Prog. Ser., 105, 31–45, doi:10.3354/meps105031, 1994.

González, H. E., Ortiz, V. C., and Sobarzo, M.: The role of faecal material in the particulate organic carbon flux in the northern Humboldt Current, Chile (23° S), before and during the 1997–1998 El Niño, J. Plankton Res., 22, 499–529, doi:10.1093/plankt/22.3.499, 2000.

González, H. E., Daneri, G., Iriarte, J. L., Yannicelli, B., Menschel, E., Barría, C., Pantoja, S., and Lizárraga, L.: Carbon fluxes within the epipelagic zone of the Humboldt Current System off Chile: The significance of euphausiids and diatoms as key functional groups for the biological pump, Progress in Oceanography, 83, 217–227, doi:10.1016/j.pocean.2009.07.036, 2009.

Guidi, L., Stemmann, L., Jackson, G. A., Ibanez, F., Claustre, H., Legendre, L., Picheral, M., and Gorsky, G.: Effects of phytoplankton community on production, size and export of large aggregates: a world-ocean analysis, Limnol. Oceanogr., 54, 1951–1963, doi:10.4319/lo.2009.54.6.1951, 2009.

Hargraves, P. E. and French, F.: Diatom resting spores: Significance and strategies, in: Survival Strategies of the Algae, edited by: Fryxell, G., Cambridge University Press, New York, 49–68, 1983.

Iversen, M. H. and Poulsen, L.: Coprorhexy, coprophagy, and coprochaly in the copepods *Calanus helgolandicus*, *Pseudocalanus elongatus*, and *Oithona similis*, Mar. Ecol.-Prog. Ser., 350, 79–89, doi:10.3354/meps07095, 2007.

Jackson, G. A., Maffione, R., Costello, D. K., Alldredge, A. L., Logan, B. E., and Dam, H. G.: Particle size spectra between 1 µm and 1 cm at Monterey Bay determined using multiple instruments, Deep-Sea Res. Pt. I, 44, 1739–1767, doi:10.1016/S0967-0637(97)00029-0, 1997.

Jackson, G. A.: A model of the formation of marine algal flocs by physical coagulation processes, Deep-Sea Res. Pt. I, 37, 1197–1211, doi:10.1016/0198-0149(90)90038-W, 1990.

Jackson, G. A.: Coagulation theory and models of oceanic plankton aggregation, in: Flocculation in Natural and Engineered Environmental Systems, CRC Press, 271–292, 2005.

Jackson, G. A., Waite, A. M., and Boyd, P. W.: Role of algal aggregation in vertical carbon export during SOIREE and in other low biomass environments, Geophys. Res. Lett., 32, L13607, doi:10.1029/2005gl023180, 2005.

Jacquet, S. H. M., Lam, P. J., Trull, T., and Dehairs, F.: Carbon export production in the sub-antarctic zone and polar front zone south of Tasmania, Deep-Sea Res. Pt. II, 58, 2277–2292, doi:10.1016/j.dsr2.2011.05.035, 2011.

Jannasch, H. W., Zafiriou, O. C., and Farrington, J. W.: A sequencing sediment trap for time-series studies of fragile particles, Limnol. Oceanogr., 25, 939–943, doi:10.4319/lo.1980.25.5.0939, 1980.

Kuwata, A. and Takahashi, M.: Life-form population responses of a marine planktonic diatom, *Chaetoceros pseudocurvisetus*, to oligotrophication in regionally upwelled water, Mar. Biol., 107, 503–512, doi:10.1007/BF01313435, 1990.

Lam, P. J. and Bishop, J. K. B.: High biomass, low export regimes in the Southern Ocean, Deep-Sea Res. Pt. II, 54, 601–638, doi:10.1016/j.dsr2.2007.01.013, 2007.

Lam, P. J., Doney, S. C., and Bishop, J. K. B.: The dynamic ocean biological pump: Insights from a global compilation of particulate organic carbon, $CaCO_3$, and opal concentration profiles from the mesopelagic, Global. Biogeochem. Cy., 25, GB3009, doi:10.1029/2010GB003868, 2011.

Lampitt, R. S., Noji, T., and Bodungen, B.: What happens to zooplankton faecal pellets? Implications for material flux, Mar. Biol., 104, 15–23, doi:10.1007/BF01313152, 1990.

Lasbleiz, M., Leblanc, K., Blain, S., Ras, J., Cornet-Barthaux, V., Hélias Nunige, S., and Quéguiner, B.: Pigments, elemental composition (C, N, P, Si) and stoichiometry of particu-

late matter, in the naturally iron fertilized region of Kerguelen in the Southern Ocean, Biogeosciences~~Discuss.~~, 11, ~~8259–8324,~~ 5931–5955, doi:10.5194/bg-11-5931-2014, 2014.

~~Laurenceau~~Laurenceau-Cornec, E. C., Trull, T. W., Davies, D., De La Rocha, C. L., and Blain, S.: Phytoplankton morphology controls on marine snow sinking velocity, Mar. Ecol.-Prog. Ser., in ~~review,~~ press, doi:10.3354/meps11116, 2014.

Lefèvre, D., Guigue, C., and Obernosterer, I.: The metabolic balance at two contrasting sites in the Southern Ocean: the iron-fertilized Kerguelen area and HNLC waters, Deep-Sea Res. Pt. II, 55, 766–776, doi:10.1016/j.dsr2.2007.12.006, 2008.

Lundsgaard, C.: Use of a high viscosity medium in studies of aggregates, in: Sediment Trap Studies in the Nordic Countries. 3. Proceeding of the Symposium on Seasonal Dynamics of Planktonic Ecosystems and Sedimentation in Coastal Nordic Waters. Finnish Environment Agency, edited by: Floderus, S., Heisakanen, A. S., Oleson, M., and Wassmann, P., Numi Print, Oy, Germany, 141–152, 1995.

Maiti, K., Charette, M. A., Buesseler, K. O., and Kahru, M.: An inverse relationship between production and export efficiency in the Southern Ocean, Geophys. Res. Lett., 40, 1557–1561, doi:10.1002/grl.50219, 2013.

Martens, P.: Faecal pellets, in: Fiches d'identification du zooplancton, edited by: Fraser, J. H., Conseil International pour l'Exploration de la Mer, 4, 1978.

Martin, J. H.: Glacial-interglacial CO_2 change: the iron hypothesis, Paleoceanography, 5, 1–13, doi:10.1029/PA005i001p00001, 1990.

Martin, J. H., Knauer, G. A., Karl, D. M., and Broenkow, W. W.: VERTEX: carbon cycling in the northeast Pacific, Deep Sea Research Part A. Oceanographic Research Papers, 34, 267–285, doi:10.1016/0198-0149(87)90086-0, 1987.

McCave, I. N.: Size spectra and aggregation of suspended particles in the deep ocean, Deep-Sea Res., 31, 329–352, doi:10.1016/0198-0149(84)90088-8, 1984.

McDonnell, A. M. P. and Buesseler, K. O.: Variability in the average sinking velocity of marine particles, Limnol. Oceanogr., 55, 2085–2096, doi:10.4319/lo.2010.55.5.2085, 2010.

Michaels, A. F. and Silver, M. W.: Primary production, sinking fluxes and the microbial food web, Deep-Sea Res., 35, 473–490, doi:10.1016/0198-0149(88)90126-4, 1988.

Morris, P. J., Sanders, R., Turnewitsch, R., and Thomalla, S.: ^{234}Th-derived particulate organic carbon export from an island-induced phytoplankton bloom in the Southern Ocean, Deep-Sea Res. Pt. II, 54, 2208–2232, doi:10.1016/j.dsr2.2007.06.002, 2007.

Mosseri, J., Quéguiner, B., Armand, L., and Cornet-Barthaux, V.: Impact of iron on silicon utilization by diatoms in the Southern Ocean: A case study of Si/N cycle decoupling in a naturally iron-enriched area, Deep-Sea Res. Pt. II, 55, 801–819, doi:10.1016/j.dsr2.2007.12.003, 2008.

Park, Y.-H., Charriaud, E., Pino, D. R., and Jeandel, C.: Seasonal and interannual variability of the mixed layer properties and steric height at station KERFIX, southwest of Kerguelen, Journal of Marine Systems, 17, 571–586, doi:10.1016/S0924-7963(98)00065-7, 1998.

Pilskaln, C. H. and Honjo, S.: The fecal pellet fraction of biogeochemical particle fluxes to the deep sea, Global. Biogeochem. Cy., 1, 31–48, doi:10.1029/GB001i001p00031, 1987.

Planchon, F., Ballas, D., Cavagna, A.-J., Bowie, A. R., Davies, D., Trull, T. W., ~~Laurenceau~~Laurenceau-Cornec, E. C., van der Merwe, P., and Dehairs, F.: Carbon export in the naturally iron-fertilized Kerguelen area of the Southern Ocean based on the ^{234}Th approach, Biogeosciences Discuss., ~~in preparation,~~ 11, 15991–16032, doi:10.5194/bgd-11-15991-2014, 2014.

Pollard, R., Sanders, R., Lucas, M., and Statham, P.: The Crozet Natural Iron Bloom and Export Experiment (CROZEX), Deep-Sea Res. Pt. II, 54, 1905–1914, doi:10.1016/j.dsr2.2007.07.023, 2007.

Quéguiner, B.: Iron fertilization and the structure of planktonic communities in high nutrient regions of the Southern Ocean, Deep-Sea Res. Pt. II, 90, 43–54, doi:10.1016/j.dsr2.2012.07.024, 2013.

Riebesell, U., Schloss, I., and Smetacek, V.: Aggregation of algae released from melting sea ice: implications for seeding and sedimentation, Polar Biol., 11, 239–248, doi:10.1007/bf00238457, 1991.

Rynearson, T. A., Richardson, K., Lampitt, R. S., Sieracki, M. E., Poulton, A. J., Lyngsgaard, M. M., and Perry, M. J.: Major contribution of diatom resting spores to vertical flux in the sub-polar North Atlantic, Deep-Sea Res. Pt. I, 82, 60–71, doi:10.1016/j.dsr.2013.07.013, 2013.

Salter, I., Lampitt, R. S., Sanders, R., Poulton, A., Kemp, A. E. S., Boorman, B., Saw, K., and Pearce, R.: Estimating carbon, silica and diatom export from a naturally fertilised phytoplankton bloom in the Southern Ocean using PELAGRA: A novel drifting sediment trap, Deep-Sea Res. Pt. II, 54, 2233–2259, doi:10.1016/j.dsr2.2007.06.008, 2007.

Salter, I., Kemp, A. E. S., Moore, C. M., Lampitt, R. S., Wolff, G. A., and Holtvoeth, J.: Diatom resting spore ecology drives enhanced carbon export from a naturally iron-fertilized bloom in the Southern Ocean, Global. Biogeochem. Cy., 26, GB1014, doi:10.1029/2010GB003977, 2012.

Savoye, N., Trull, T. W., Jacquet, S. H. M., Navez, J., and Dehairs, F.: ^{234}Th-based export fluxes during a natural iron fertilization experiment in the Southern Ocean (KEOPS), Deep-Sea Res. Pt. II, 55, 841–855, doi:10.1016/j.dsr2.2007.12.036, 2008.

Sigman, D. M. and Boyle, E. A.: Glacial/interglacial variations in atmospheric carbon dioxide, Nature, 407, 859–869, doi:10.1038/35038000, 2000.

Silver, M. W. and Gowing, M. M.: The "Particle" Flux: origins and biological components, Prog. Oceanogr., 26, 75–113, doi:10.1016/0079-6611(91)90007-9, 1991.

Small, L. F., Fowler, S. W., and Ünlü, M. Y.: Sinking rates of natural copepod fecal pellets, Mar. Biol., 51, 233–241, doi:10.1007/BF00386803, 1979.

Smetacek, V., Klaas, C., Strass, V. H., Assmy, P., Montresor, M., Cisewski, B., Savoye, N., Webb, A., d'Ovidio, F., Arrieta, J. M., Bathmann, U., Bellerby, R., Berg, G. M., Croot, P., Gonzalez, S., Henjes, J., Herndl, G. J., Hoffmann, L. J., Leach, H., Losch, M., Mills, M. M., Neill, C., Peeken, I., Rottgers, R., Sachs, O., Sauter, E., Schmidt, M. M., Schwarz, J., Terbruggen, A., and Wolf-Gladrow, D.: Deep carbon export from a Southern Ocean iron-fertilized diatom bloom, Nature, 487, 313–319, doi:10.1038/nature11229, 2012.

Suess, E.: Particulate organic carbon flux in the oceans – surface productivity and oxygen utilization, Nature, 288, 260–263, doi:10.1038/288260a0, 1980.

Suzuki, H., Sasaki, H., and Fukuchi, M.: Loss processes of sinking fecal pellets of zooplankton in the mesopelagic layers of the Antarctic Marginal Ice Zone, J. Oceanogr., 59, 809–818, doi:10.1023/B:JOCE.0000009572.08048.0d, 2003.

Trull, T. W., Bray, S. G., Buesseler, K. O., Lamborg, C. H., Manganini, S., Moy, C., and Valdes, J.: In situ measurement of mesopelagic particle sinking rates and the control of carbon transfer to the ocean interior during the Vertical Flux in the Global Ocean (VERTIGO) voyages in the North Pacific, Deep-Sea Res. Pt. II, 55, 1684–1695, doi:10.1016/j.dsr2.2008.04.021, 2008.

Trull, T. W., Davies, D. M., Dehairs, F., Cavagna, A.-J., Lasbleiz, M., Laurenceau-Cornec, E. C., d'Ovidio, F., Planchon, F., Leblanc, K., Quéguiner, B., and Blain, S.: Chemometric perspectives on plankton community responses to natural iron fertilization over and downstream of the Kerguelen Plateau in the Southern Ocean, Biogeosciences Discuss., 11, 13841–13903, doi:10.5194/bgd-11-13841-2014, 2014.

Turner, J. T.: Zooplankton fecal pellets, marine snow and sinking phytoplankton blooms, Aquat. Microb. Ecol., 27, 57–102, doi:10.3354/ame027057, 2002.

Urban-Rich, J., Hansell, D. A., and Roman, M. R.: Analysis of copepod fecal pellet carbon using a high temperature combustion method, Mar. Ecol.-Prog. Ser., 171, 199–208, doi:10.3354/meps171199, 1998.

Volk, T. and Hoffert, M. I.: Ocean carbon pumps: Analysis of relative strengths and efficiencies in ocean-driven atmospheric CO_2 changes, in: The Carbon Cycle and Atmospheric CO_2: Natural Variations Archean to Present, edited by: Sundquist, E. T. and Broecker, W. S., AGU, Washington, DC, 99–110, 1985.

Waite, A. M. and Nodder, S. D.: The effect of in situ iron addition on the sinking rates and export flux of Southern Ocean diatoms, Deep-Sea Res. Pt. II, 48, 2635–2654, doi:10.1016/S0967-0645(01)00012-1, 2001.

Wallace, M. I., Cottier, F. R., Brierley, A. S., and Tarling, G. A.: Modelling the influence of copepod behaviour on faecal pellet export at high latitudes, Polar Biol., 36, 579–592, doi:10.1007/s00300-013-1287-7, 2013.

Wassmann, P.: Relationship between primary and export production in the boreal coastal zone of the North Atlantic, Limnol. Oceanogr., 35, 464–471, doi:10.4319/lo.1990.35.2.0464, 1990.

Wassmann, P.: Retention vs. export food chains: processes controlling sinking loss from marine pelagic systems, Hydrobiologia, 363, 29–57, doi:10.1023/A:1003113403096, 1998.

Wassmann, P., Ypma, J. E., and Tselepides, A.: Vertical flux of faecal pellets and microplankton on the shelf of the oligotrophic Cretan Sea (NE Mediterranean Sea), Prog. Oceanogr., 46, 241–258, doi:10.1016/S0079-6611(00)00021-5, 2000.

Wiebe, P. H., Burt, K. H., Boyd, S. H., and Morton, A. W.: A multiple opening/closing net and environment sensing system for sampling zooplankton, J. Mar. Res., 34, 313–326, 1976.

Wiebe, P., Boyd, S., Davis, B., and Cox, J.: Avoidance of towed nets by the euphausiid *Nematoscelis megalops*, Fish. B-NOAA, 80, 75–91, 1982.

Yoon, W., Kim, S., and Han, K.: Morphology and sinking velocities of fecal pellets of copepod, molluscan, euphausiid, and salp taxa in the northeastern tropical Atlantic, Mar. Biol., 139, 923–928, doi:10.1007/s002270100630, 2001.

Zhou, M., Zhu, Y., d'Ovidio, F., Park, Y.-H., Durand, I., Kestenare, E., Sanial, V., Van-Beek, P., Queguiner, B., Carlotti, F., and Blain, S.: Surface currents and upwelling in Kerguelen Plateau regions, Biogeosciences Discuss., 11, 6845–6876, doi:10.5194/bgd-11-6845-2014, 2014.

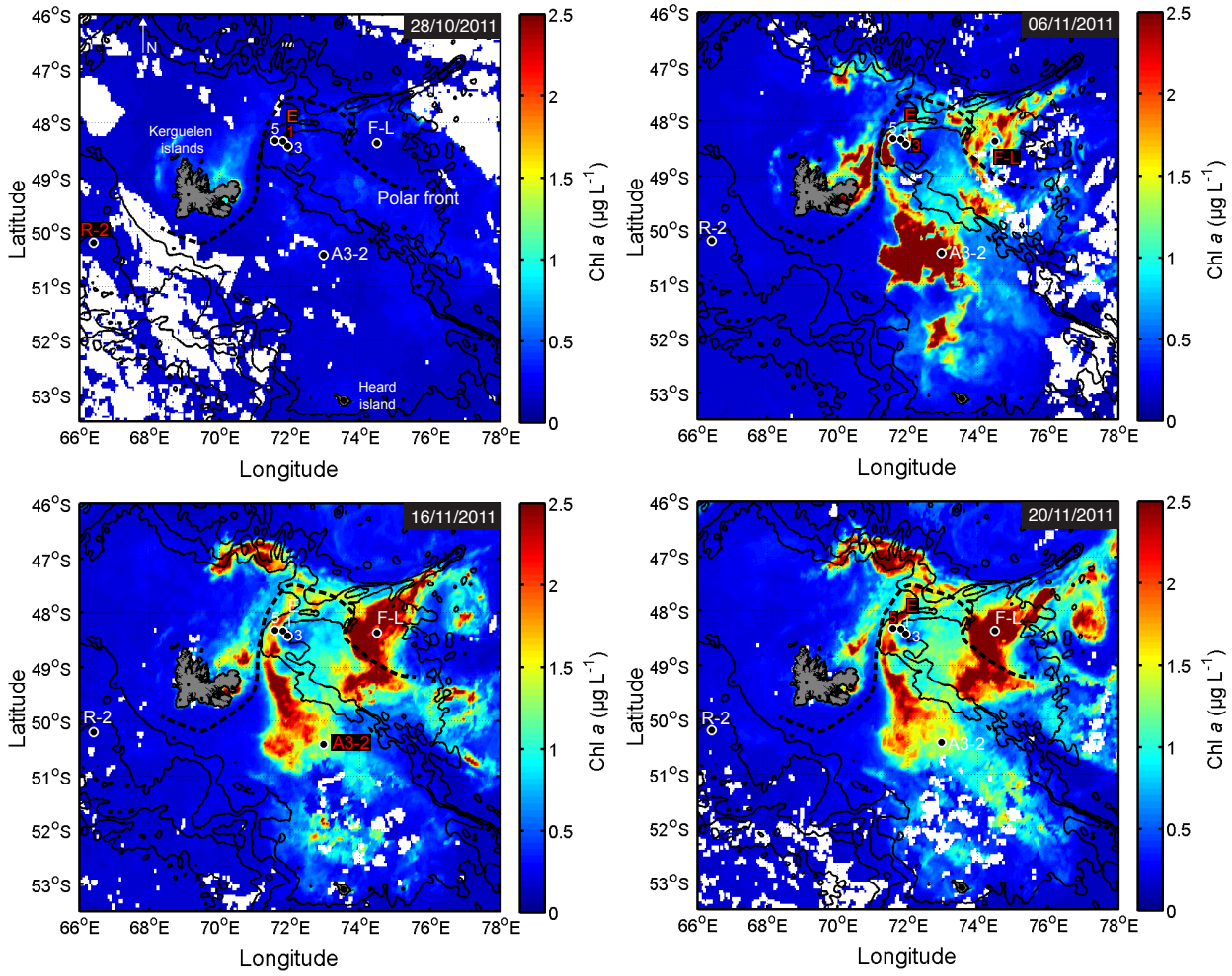

Figure 1. MODIS-Aqua satellite (CLS-CNES) images of surface chlorophyll *a* concentration (Chl *a*) at different bloom stages from the 28 October to the 20 November 2011. Images show free-drifting sediment trap deployment locations in contrasted biomass levels. On each map, red i.d. represent the station(s) sampled at the date of the map $\pm$3 days.

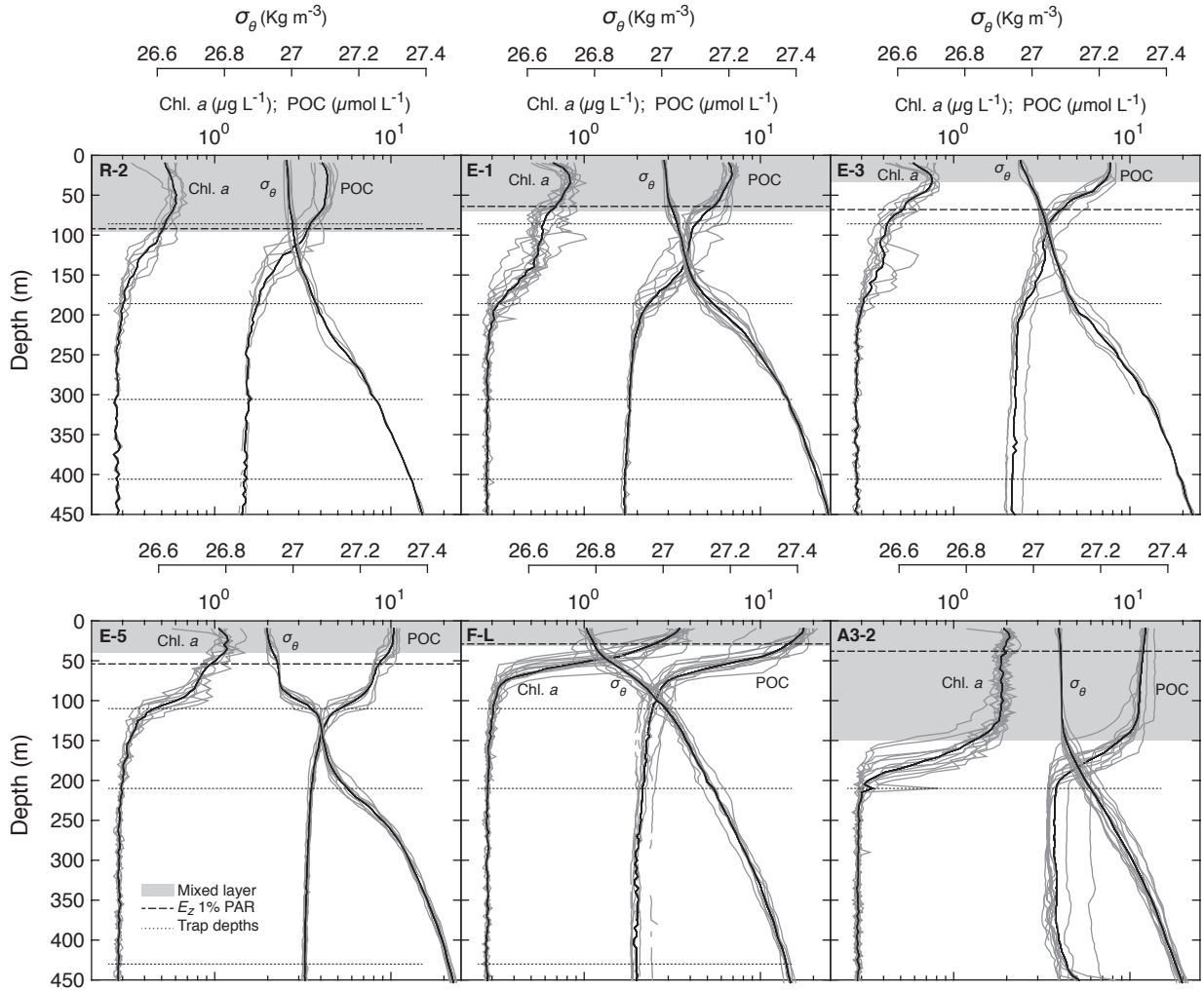

Figure 2. Water column properties and biomass at each site. ~~Fluo~~Chl. *a*: ~~fluorescence~~ chlorophyll *a* (µg L^{-1}); $\mathcal{T}\sigma_\theta$: ~~temperature~~ potential density anomaly (~~C~~Kg m^{-3}); POC: particulate organic carbon (µmol L^{-1}). Gray lines indicate CTD profiles and black lines represent their average values. E_Z 1 % PAR: base of the euphotic zone assumed at 1 % of the photosynthetic available radiation (PAR).

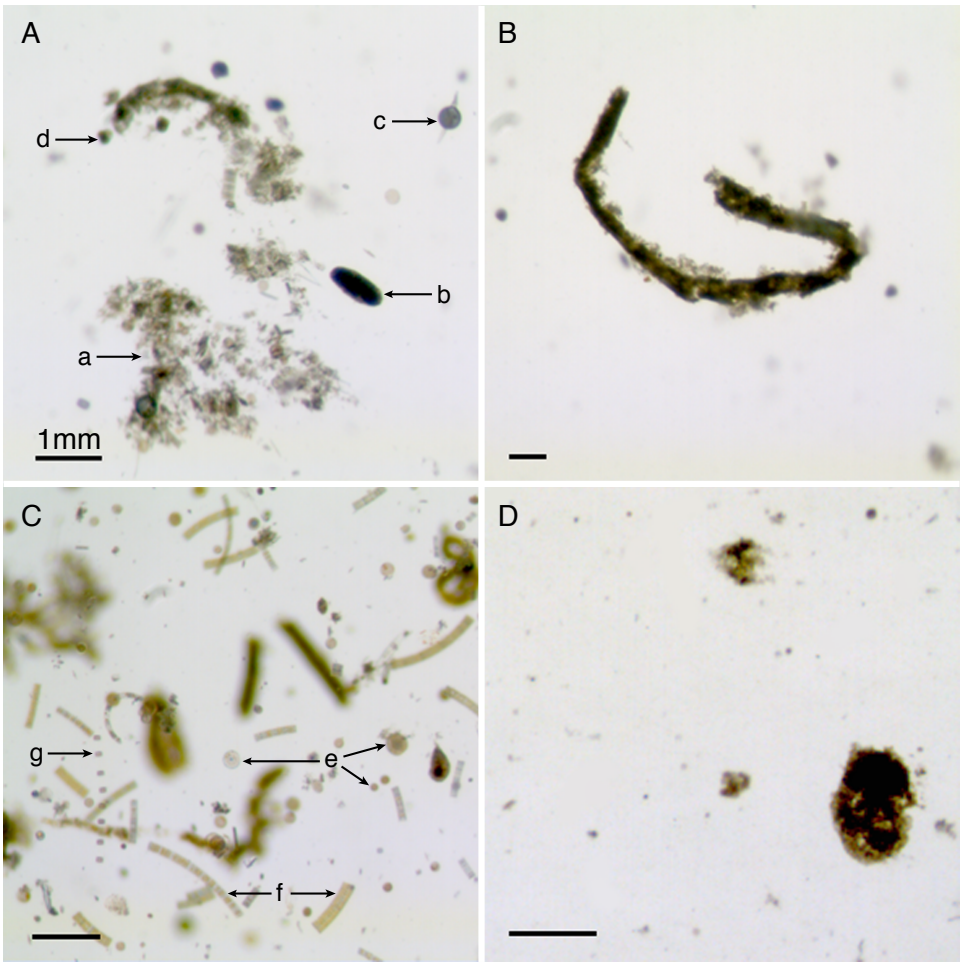

Figure 3. High resolution pictures of particles embedded in polyacrylamide gels showing the main categories of particles collected. **(A)** phytodetrital aggregate (a), oval fecal pellet (b), radiolarian (c), foraminifera (d); **(B)** large cylindrical fecal pellet; **(C)** small and large centric diatom single cells (e), chains of pennate diatoms of the genera *Fragilariopsis* spp. (f), chain of small centric diatom cells (g); **(D)** fecal aggregate. Note the difference of compactness and optical density between phytodetrital and fecal aggregates.

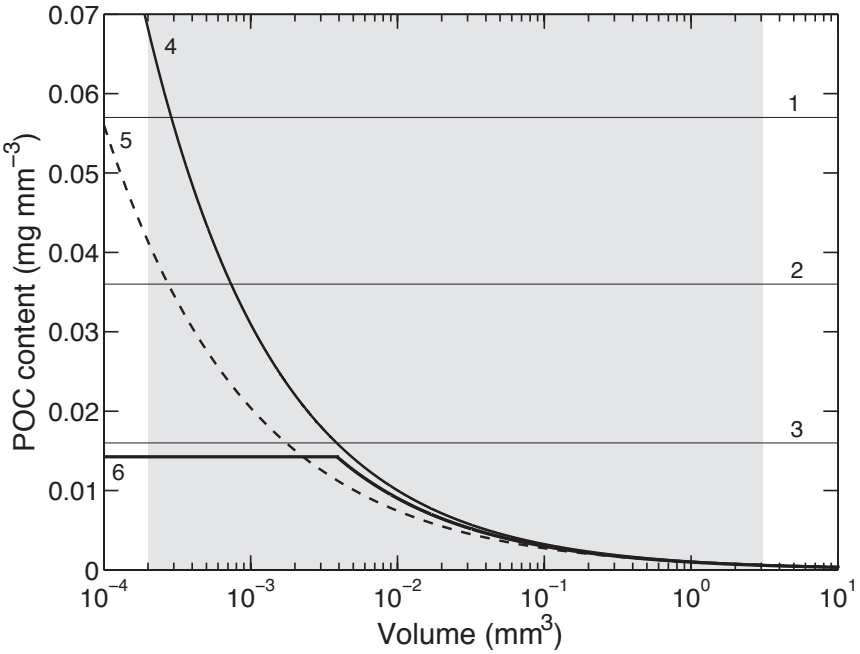

Figure 4. Empirical relationships of particulate organic carbon (POC) content as a function of volume for different categories of sinking particles. 1, 2 and 3: copepod fecal pellets, average of euphausiids and copepod fecal pellets and euphausiids fecal pellets respectively (González and Smetacek, 1994); 4: fecal marine snow (Alldredge, 1998); 5: diatom marine snow (Alldredge, 1998); 6: small and large aggregates (*sensu lato*) respectively (Ebersbach and Trull, 2008). Grey area represents the size range of particles processed in this study. Note the constant carbon mass per unit volume in fecal pellets based on solid geometry (linear relationship) and its decrease with increasing volume scaled on fractal geometry (power relationship) in the case of aggregates.

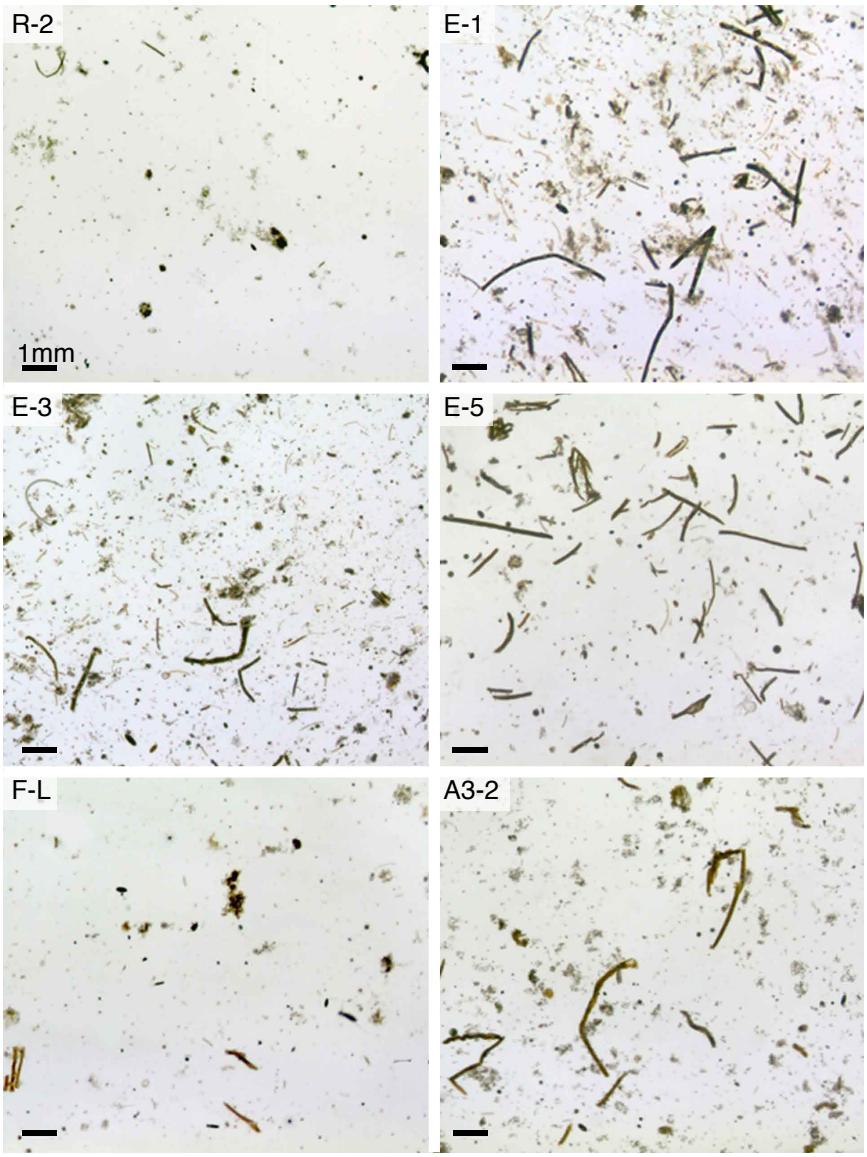

Figure 5. Images of sinking particles embedded in polyacrylamide gels, collected at each site at 210 m. Comparison of images suggest differences in term of particles abundance and nature at each site.

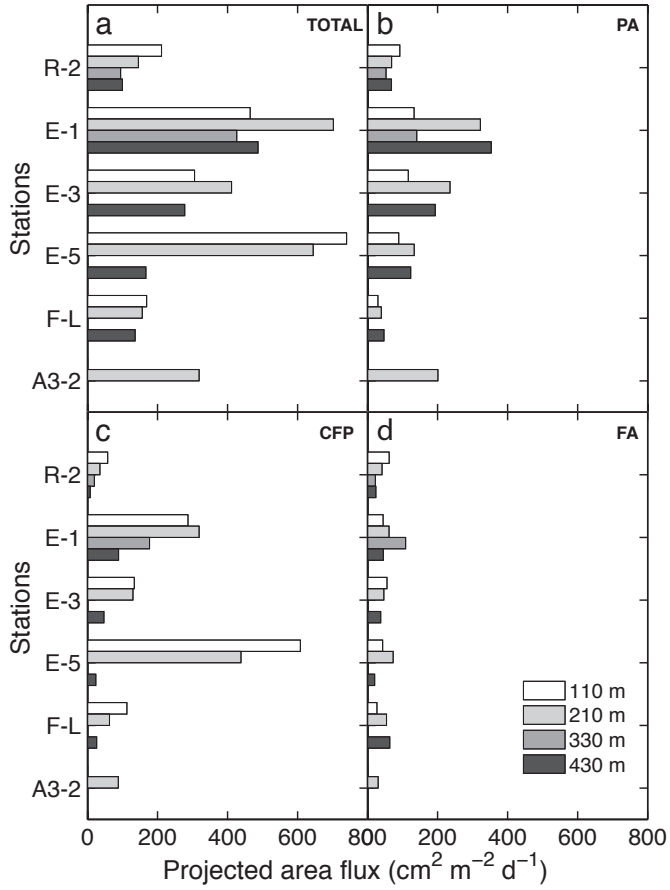

Figure 6. Projected area of particles estimated from image analysis at each site and depth and expressed as fluxes ($cm^2\,m^{-2}\,d^{-1}$). **(a)** All particles (TOTAL); **(b)** phytodetrital aggregates (PA); **(c)** cylindrical fecal pellets (CFP); **(d)** fecal aggregates (FA). The figure suggests a sinking flux dominated by cylindrical fecal pellets at the surface, except at R-2 where phytodetrital aggregates represented the most important fraction. The attenuation of the cylindrical fecal pellet flux with depth observable at all stations was combined with an increase of the flux of phytodetrital and fecal aggregates at almost all stations. At 430 m, phytodetrital aggregates were then the most dominant particles.

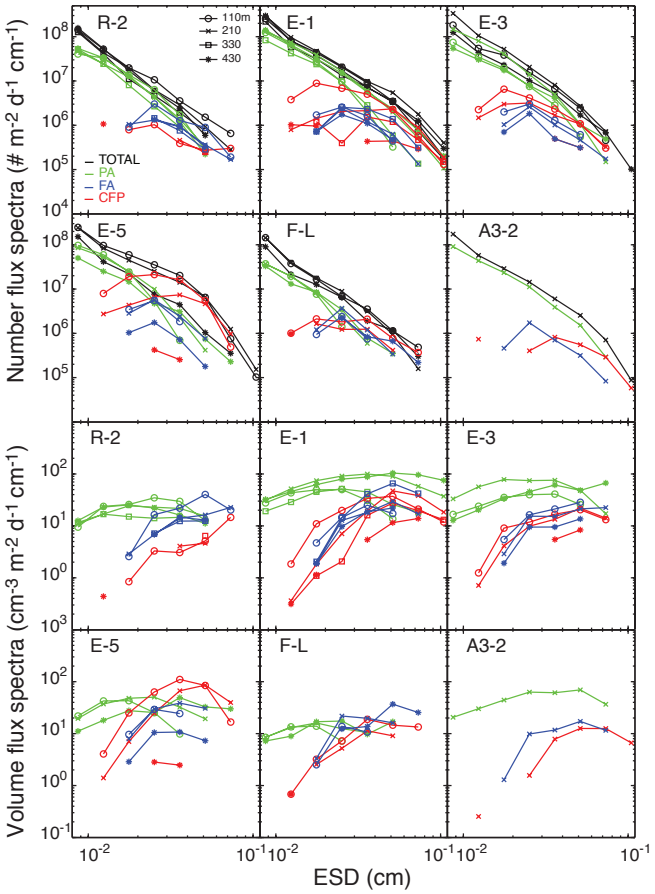

Figure 7. Total number and volume fluxes of particles binned in 10 size classes. Bins with less than 5 particles were removed (see Table 2 and text for explanations). Results are shown for each category of particles at all depths and sites. TOTAL: all particles; PA: phytodetrital aggregates; FA: fecal aggregates; CFP: cylindrical fecal pellets. Smallest particles represented by phytodetrital aggregates were the most numerous at every site and depth. Middle sized phytodetrital aggregates and fecal particles (pellets and aggregates) contributed the most to the volume flux due to the overall rarity of very large particles relative to all particles.

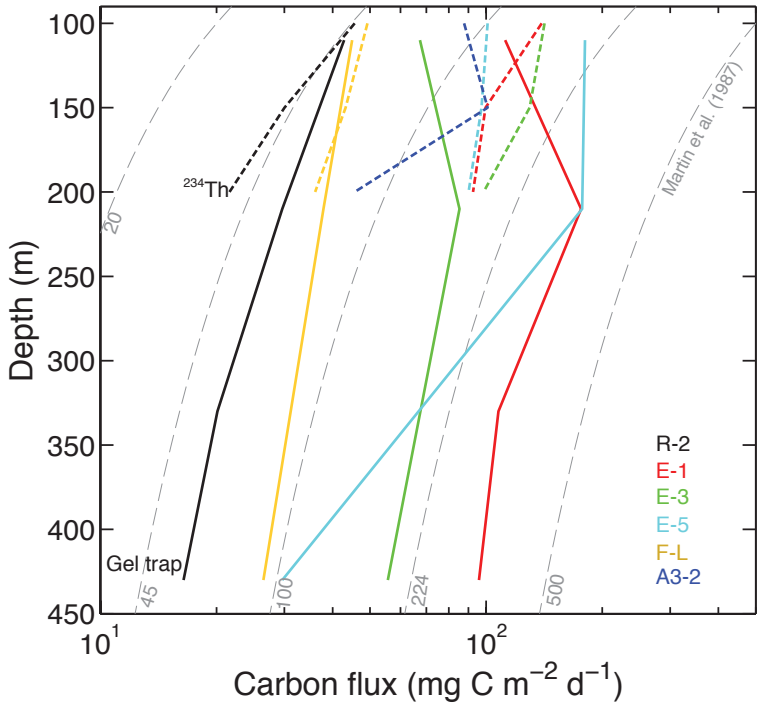

Figure 8. Variation of the carbon flux with depth estimated from gel trap and ^{234}Th methods. The empirical attenuation of the flux with depth (Martin curve) is represented in grey dash lines for initial values of the carbon flux at 100 m from 20 to 500 mg C m^{-2} d^{-1}. Results show overall poor agreements between observed fluxes and the Martin curve suggesting the complexity of the processes affecting the carbon flux with depth.

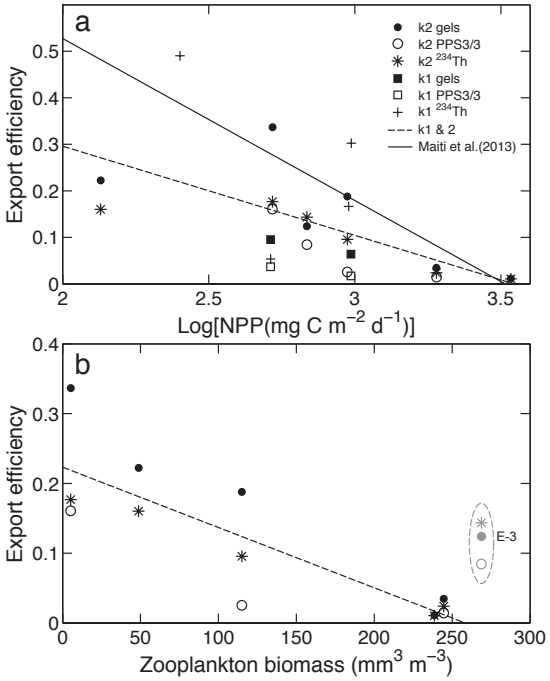

Figure 9. Relationships between net primary productivity **(a)**, zooplankton biomass **(b)** and export efficiency calculated using particulate organic carbon fluxes estimated at 200 ± 10 m from PPS3/3 traps, gel traps and ^{234}Th methods for the KEOPS2 (k2) and KEOPS1 (k1; **(a)** only) studies. **(a)** The black line represents the empirical relationship from Maiti et al. (2013) estimated in the Southern Ocean ($y = -0.35x + 1.22$; $r^2 = 0.97$); dash line represents the regression line for all KEOPS data ($y = -0.19x + 0.68$; $n = 24$, $r^2 = 0.33$, $p < 0.005$). **(b)** Dash line represents the regression line for KEOPS2 data ($y = -0.00086x + 0.2232$; $n = 15$, $r^2 = 0.72$, $p < 0.0005$). E-3 was assumed an outlier and was excluded from the best fit calculation (see text for possible explanation). **(a)** Suggests that the most productive sites are the less efficient to export carbon. **(b)** Suggests that zooplankton biomass could influence the efficiency of carbon export by by-passing direct export via phytodetrital aggregates.